POSS-BASED CARBON FIBER TREATMENT FOR ENHANCED STRENGTH AND TOUGHNESS OF COMPOSITES

By

BLAZE ALLAN HECKERT

Bachelor of Science in Biology
Pittsburg State University
Pittsburg, Kansas, USA
2015

Master of Science in Polymer Chemistry
Pittsburg State University
Pittsburg, Kansas, USA
2016

Submitted to the Faculty of the
Graduate College of
Oklahoma State University
in partial fulfillment of
the requirements for
the Degree of
Doctor of Philosophy
July, 2020

POSS-BASED CARBON FIBER TREATMENT FOR ENHANCED STRENGTH AND TOUGHNESS OF COMPOSITES

Committee Members:

Dr. Raman P. Singh

Dissertation Advisor

Dr. K. Ranji Vaidyanathan

Dr. James E. Smay

Dr. Khaled A. Sallam

ACKNOWLEDGMENTS

Firstly, I am grateful to God for the blessings he has provided that allowed me to pursue this PhD and arranging such great individuals to guide and motivate me along the way.

I am extremely grateful to my advisor, Dr. Raman Singh, for his encouragement and support which has been consistent from my first day. I approached you with a severe lack of education in this particular area, instead of seeing this as a negative and time consuming undertaking, you used my different background to expand into new areas. I am deeply indebted for this opportunity and the financial support you have given me in this pursuit. I truly hope this will bring the lab new opportunities in the future.

To my lab-mates, fellow students, and everyone at the HRC that have helped me throughout this work. You all were instrumental in helping me with this accomplishment. I hope to maintain these friendships throughout the next chapter of my life.

To my committee members, Dr. Ranji Vaidyanathan, Dr. Jim Smay, and Dr. Khaled Sallam, thank you for helping guide me through this experience. Your guidance and feedback along the way were critical to my success.

Lastly, I am very thankful for the love and support of my wife Deaven for helping me to stay focused and standing by my side through out this accomplishment. The decision to get married, move states and begin a PhD program was a whirlwind of a summer and I couldn't imagine doing it with anyone else. The ability to pursue and complete this degree would not have been possible without the support of my mother and grandparents. From the very first talks of pursuing this degree to the commencement of this dissertation, your belief in me and generosity has made this experience such an enjoyable one. You have given me the best shot at life and there is no repaying such a gift, thank you. To the rest of my family, my in-laws and the many friends I have gained while at OSU, thank you all for the support, the memories and the friendships, I carry all of these with me.

Acknowledgments reflect the views of the author and are not endorsed by committee members or Oklahoma State University.

Name: Blaze Allan Heckert

Date of Degree: July, 2020

Title of Study: POSS-BASED CARBON FIBER TREATMENT FOR ENHANCED STRENGTH AND TOUGHNESS OF COMPOSITES

Major Field: Materials Science and Engineering

In this study, two techniques are used to coat carbon fibers with polyhedral oligomeric silsesquioxane (POSS) as a fiber surface treatment. This process utilizes the unique organic–inorganic hybrid structure of POSS to develop damage–tolerant composite laminates. This paper compares POSS—based treatments based on two different approaches. A more traditional approach via esterification reaction and a novel approach utilizing thiol-ene click chemistry. Click chemistry reactions achieve very high yields and are performed in a variety of solvents.

The treated carbon fibers are analyzed using XPS and SEM. The modified POSS used in the first approach is characterized using NMR and FT-IR. Single fiber tensile tests of the first approach show a significant decrease in the fiber tensile strength, while the second approach showed no loss in fiber strength. Interfacial shear strength is determined using single-fiber fragmentation testing. The first approach showed a decrease of 24% in the fiber fragmentation length compared to the as-received fibers, however because of the loss in fiber strength there is a decrease of 6% in the interfacial shear strength compared to the as-received carbon fibers. The second approach, however, shows a 27% decrease in the fiber fragment length compared to the as-received fibers, and as a result has an 71% increase in the interfacial shear strength as compared to the as-received carbon fibers and a 80% increase compared to the first approach.

There has been recent interest in the use of multilayer POSS to further enhance the interfacial properties of the composite. However, this comes with the challenge of POSS–POSS agglomeration that will result in nonuniform distribution of properties across the fiber surface. There has been no attempt to control the POSS–POSS, nor to examine how the compliance will be altered by additional layers of POSS. To better understand how additional POSS layers can alter the compliance of the interface, different POSS networks were synthesized using hexane-1,6-dithiol as a linking molecule and thiol-ene click chemistry. These networks varied by POSS density using different ratios of the dithiol linker molecule. The properties of these networks were analyzed using SEM and XRF.

TABLE OF CONTENTS

LIST OF TABLES

Table Page

LIST OF FIGURES

Figure Page

List of Symbols

ν	Poisson's Ratio
σ_0	Fiber strength under no load
σ_c	Fiber strength at the critical fiber fragmentation length
σ_f	Fiber tensile strength
τ	Interfacial shear strength
A	Cross-sectional area of the fiber
C	Shear modulus
C^f	Shear modulus of the fiber
C^i	Shear modulus of the interphase region
C^m	Shear modulus of the matrix
C^p	Shear modulus of POSS networks
d	Fiber diameter
E	Elastic modulus
l_c	Critical fiber fragmentation length
l_f	Fiber gauge length
m	Weibull modulus
$p(\sigma)$	Probability of fiber failure

P_f Load at which the fiber breaks

r_f Radius of the carbon fiber

r_i Radius of the interphase region

CHAPTER I

Introduction

Carbon fiber polymer composites have become mainstream in aerospace and automotive industries [1, 2], due to the exceptional properties such as high specific strength and stiffness [3–5]. The fiber-matrix interface has significant influence over the mechanical properties of composites [6]. A properly constructed interface can enhance the mechanical properties of a composite by relieving internal stress concentrations [7]. Nonetheless, due to the relatively *chemically inert* and *smooth* surface of carbon fibers [8], the *inherent* interfacial adhesion between the fiber and matrix is weak. To address this shortcoming, numerous methods have been developed to promote adhesion between the fiber and matrix material. Methods include chemical oxidation [6, 8, 9], fiber sizings [1, 10, 11], and in recent years the inclusion of nanoparticles within the interphase region [12–14]. In particular, these nanoparticles have functional groups that can react with the functional groups available in the matrix molecules [15].

The improvement of both strength and toughness in composite materials is reliant on the construction of the interface. It is often the case that one of these, either strength or toughness, is improved at the expense of the other. While a well-bonded interface is critical to improve both properties, a strong composite typically requires a stiff interface, while improving the toughness of the composite requires a more compliant domain [16–19]. In recent years, hybrid molecules that have both rigid and compliant characteristics have been utilized as a fiber treatment. This work focuses on the development of a carbon fiber surface treatment utilizing a highly selective chemistry to build controlled networks. The density of these networks will be used to control the stiffness of the interface and optimize the

strength and toughness of the composites.

1.1 Literature review of fiber surface treatments

1.1.1 Chemical oxidation

Motivated by the many advantages that come with carbon fiber as the reinforcement phase in composites, many researchers have explored ways to improve the physicochemical interactions between the fiber and matrix. A variety of treatments have been developed. The treatments can generally be characterized as dry gaseous plasma treatments, wet chemical acid treatments, or multi-scale nanoscale filler coatings [6, 8, 9]. All of these treatments can increase the fiber-matrix adhesion leading to a more robust composite. However, the harsh environment produced from the gaseous plasma and chemical acid treatments can cause significant damage to the fibers in the form of pitting and deep etching across the fiber surface, degrading the mechanical properties of the fibers. As an example, Tiwari *et al.* examined the effect of chemical oxidation using sulfuric acid and found a decrease in fiber tensile strength of 49.2% after 120 minutes of treatment [20]. The results are shown below in Figure 1.1. Loss in fiber tensile strength limits the mechanical properties of the resulting composite, especially in the fiber-dominated direction. To address this limitation, researchers have investigated more complex multi-scale treatments using nanomaterials.

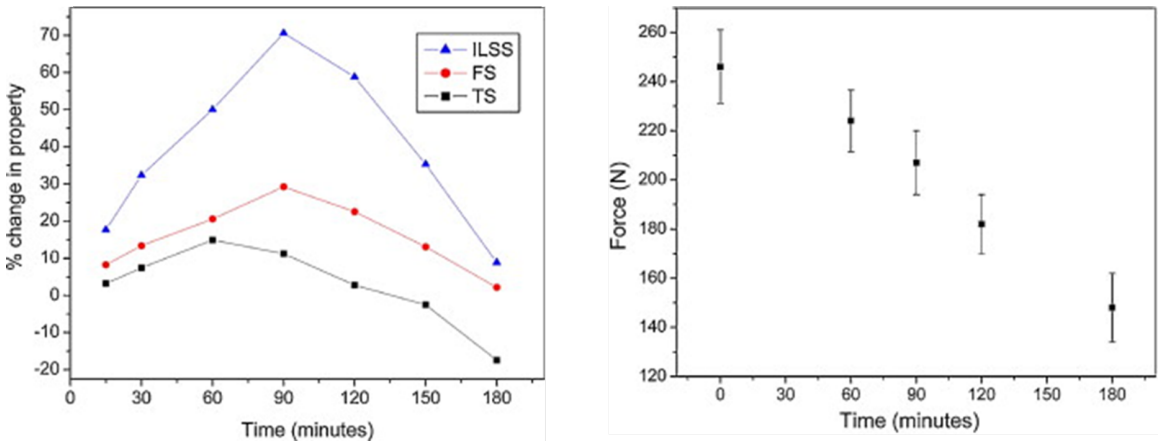

Figure 1.1: Effect of chemical oxidation on carbon fibers. Taken from Tiwari *et al.* [20].

1.1.2 Nanoparticle carbon fiber surface treatments

Nanomaterials provide a variety of benefits in the construction of an interface between carbon fibers and polymer matrices. Depending on the nanomaterial, it can greatly increase the compatibility with the resin material, improve the stress transferability and adhesion between fiber and matrix. All of these significantly improve the overall mechanical properties of the composite [14]. Common nanomaterials used include carbon nanotubes (CNTs) and graphene. The high tensile modulus and tensile strength, 1 TPa and 100 GPa, respectively, of the CNTs and graphene, made them promising materials for lightweight and exceptionally strong material applications [21–23]. Along with this, CNTs and graphene, when used as a reinforcing material within the interphase, promote better mechanical interlocking with the resin material and, when modified before use, can chemically react with both the fiber surface and matrix material [13, 24, 25]. Bekyarova *et al.* in 2007 compared the change in shear strength between oxidized carbon fibers epoxy composites and carbon nanotube functionalized carbon fiber epoxy composites. The shear strength values are shown below in Figure 2.1, and the CNT functionalized carbon fiber composites saw enhancements of 20% and 40% for CNT loading weights of 0.2 and 0.5 wt% respectively [26].

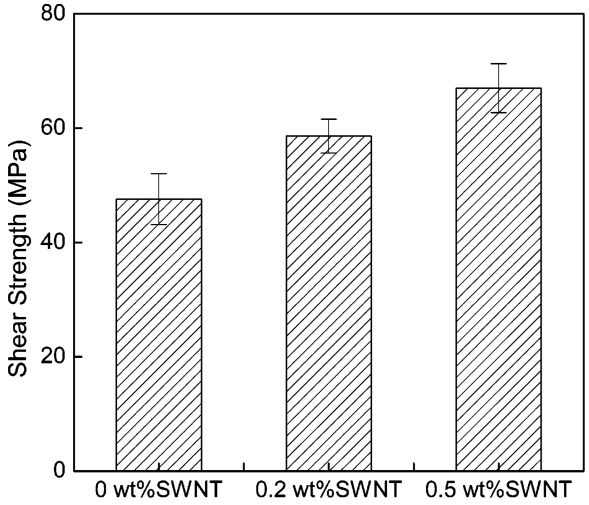

Figure 1.2: Shear strength of carbon fiber-epoxy composites with and without CNTs. Taken from Bekyarova *et al.* [26].

This study demonstrated it is possible to achieve a significant increase in mechanical properties using carbon nanotubes on the functionalized carbon fiber surface. However, as CNT wt% is increased further, properties are often found to deteriorate. This is due to the tendency of CNTs to agglomerate at relatively low loading weights. For example, Lau *et al.* found that with a two wt% incorporation of carbon nanotubes, there was a decrease in both the flexural strength and stiffness of the resulting composite compared to that of neat epoxy [27]. Along with this, carbon-based nanomaterials require prior chemical treatment, much like carbon fibers. This is because they are also chemically smooth and inert [28,29].

The exceptional stiffness of carbon based-nanomaterials is one of the reasons they have shown to significantly improve the mechanical properties of composites when used as a nanofiller reinforcement. This same stiffness may not yield the same overall improvement when applied to the interface of a carbon fiber-epoxy composite. Deng *et al.* in 2013 studied the fracture toughness of a composite based on improvements in interfacial toughening [18]. The study reported that an overly stiff interface that is tightly bound to both the carbon fiber and matrix material significantly reduces the overall impact toughness. It was explained that a flexible interlayer could accommodate larger deformations and relax stress concentrations that build at the interface, act as a crack arrester preventing propagation, and also allow more overall deformation before failure. These mechanisms delay material damage and prolong the life of the composite.

Finally, there is also a great deal of risk to the researchers while handling carbon-based nanomaterials. The Center for Disease Control (CDC) has reported that these materials, including CNTs, could cause adverse pulmonary effects. These effects, when compared to other fibrogenic materials (silica, asbestos, etc.), were shown to have a similar or greater potency [30–32].

These studies have shown that carbon-based nanomaterials can be used to create strong composite materials. However, the durability can be compromised when these materials are used as an interfacial treatment on carbon fibers from a lack of flexibility within the

interfacial region. An ideal material would provide strong interfacial adhesion while having a degree of compliance to relax built-up stress concentrations without causing catastrophic failure of the material. A relatively new material, known as polyhedral oligomeric silsesquioxane (POSS), has emerged as a promising nanofiller. If POSS is instead used to construct an interfacial layer rather than as a filler material in polymer composites its unique structure may provide both strength and compliance. POSS is also a liquid-based material and does not have the safety concerns associated with CNTs or other carbon based nanomaterials.

1.2 Polyhedral oligomeric silsesquioxane (POSS)

Polyhedral oligomeric silsesquioxane (POSS) is a unique hybrid nanomaterial possessing eight organic functional groups that surround an inorganic silicon-oxygen cage-like core [33–35], as shown below in Figure 2.2. The eight external groups give POSS many benefits, including compatibility with many matrix materials, sites for further reactions, and a degree of compliance to the molecule. The silicon–oxygen cage that makes up the core of the POSS molecule is rigid and would help provide strength to the fiber-matrix interfacial layer.

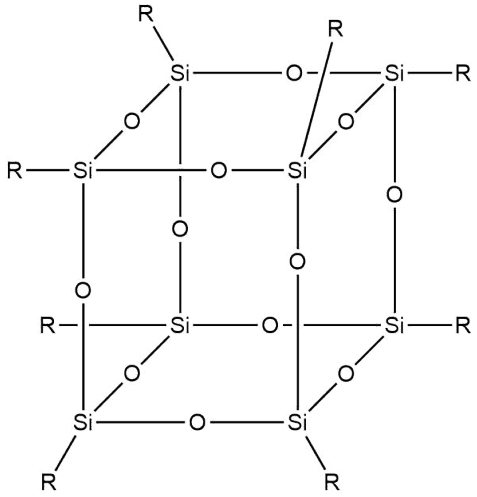

Figure 1.3: Polyhedral oligomeric silsesquioxane with generic functional groups, drawn using ChemDraw.

Researchers have shown the benefits of including POSS cages into a polymeric composite as a nanofiller. There is an increase in strength, rigidity as well as impact resistance [7, 36]. In 2017 Mishra *et al.* studied the effect of varying the loading weight and functional group of POSS inclusion within epoxy resin [37]. They found an increase in fracture toughness by a factor of 2.3 with the inclusion of glycidyl-POSS, though only an increase of 1.3 with the inclusion of the trisilanol phenyl-POSS both at a 5 wt% loading. In 2019, Mishra *et al.* used the same glycidyl-POSS at 5 wt% loading and found an improvement of 70% in the interlaminar fracture toughness [38]. These improvements were attributed directly to the chemical compatibility of the POSS structure and the enhanced adhesion between the fiber and resin material. However, at higher loading wt%, the strength of the resulting composite materials were diminished and the failure mode changes from brittle to ductile. This was attributed to POSS–POSS self-assembly creating areas with a high degree of compliance. This nonuniform distribution of properties results in limited benefit to both the toughness and strength of the POSS-nanocomposite.

There have been a limited number of studies that looked at the inclusion of POSS into the interface of carbon fiber composites, but all have shown significant increases in the

interfacial properties [12, 39, 40]. Wu *et al.* chemically grafted amino-POSS to the surface of carbon fibers, this was done using a series of reactions including oxidation of carbon fibers and using a bridge molecule to link the POSS to the surface [41]. The interfacial shear strength and impact resistance increased 41% and 35%, respectively. However, as mentioned earlier, the chemical oxidation of carbon fibers can reduce the tensile strength and limit the overall mechanical properties of the composite. This is similar to most studies that have focused on chemical modification of the carbon fiber or POSS molecule to achieve a successful functionalization, creating a coating of POSS on the carbon fiber.

The benefits could be exponentially improved upon, however, if multiple POSS molecules could be connected in a controlled manner [12]. Ma *et al.* in 2019 utilized a dendrimer type approach to building multiple generations of POSS along the surface of the carbon fiber. This approach required modification of both the carbon fiber and POSS molecule before the first layer of POSS could be graft to the carbon fiber surface. Each new generation required two-step modification of the next POSS molecule before reaction with the first layer of POSS. The results of this study showed that increasing the number of layers of POSS led to an increase in the interfacial properties. The interfacial shear strength of the monolayer POSS carbon fiber saw an increase of 46% as compared to the as-received carbon fibers, and with a third-generation POSS an increase of 75% compared to the as-received carbon fibers. The type of chemistry used by Ma *et al.* to build the POSS network along the surface of the carbon fiber however is not ideal for a uniform coating. The amine alkylation reaction used is shown to have poor yields, Werner *et al.* reports only a 10–30% yield [42]. A more efficient chemistry could result in a far greater increase in the interfacial properties.

One type of chemistry known to be highly efficient and highly versatile is known as click chemistry. These click reactions were born from the premise that organic synthesis should focus on highly selective and neat reactions, meaning no or limited side products formed, and occur under mild conditions. For this study click reactions can provide uniform coating, easy cleanup, and minimize degradation of the fiber due to the mild reaction

environment [43]. Although there are different variants of these click reactions, the reaction between an alkene and thiol is the most viable due to the commercial availability of octavinyl-POSS. This reaction will be explained in greater detail during the functionalization process.

1.3 Motivation for this study

The goal of this research is to improve the strength and toughness of carbon fiber reinforced polymer composites. This will be accomplished through controlled application of POSS on the fiber surface. The first POSS coating will focus on utilizing click chemistry to achieve a more complete coverage of the fiber and limit localized points of failure. A more common approach to POSS coating, utilizing ester reaction as the method of reaction between fiber and POSS, will be synthesized along side our click-based chemistry approach. These fiber treatments are characterized mechanically and chemically to determine the effectiveness of the treatments. Chemical characterization will be done using XPS which analyzes the chemical composition of the surface. The surface of the carbon fibers will be examined using scanning electron microscopy/Energy Dispersive X-Ray Spectroscopy (SEM/EDS) and allow the effects of the treatments to be monitored visually and surface chemical composition mapped. The effect of these treatments on the mechanical and interfacial properties will be examined using single-fiber tensile and single-fiber fragmentation testing, respectively. Lastly, because of the number of functional groups present on POSS, researchers have begun utilizing multiple layers of POSS as a surface treatment. The results so far have shown a continual increase in the interfacial shear strength with increasing number of POSS layers, but few studies utilize more than a third POSS layer. To better understand how multiple controlled layers of POSS will impact the properties of the composite, several POSS–POSS networks were synthesized and the modulus of these networks will be analyzed using atomic force microscopy (AFM). These networks give some representation of what to expect as multiple layers are constructed on the surface of the carbon fiber.

CHAPTER II

Functionalization of Carbon Fiber Surface

There are a variety of click reactions that have emerged over the last century, with the copper-catalyzed azide and alkyne click reaction having received the most use in areas such as medical, hydrogel, and dendrimer synthesis, demonstrating the extensive application of such reactions [44–46]. However, this set of clickable functionalities is difficult to produce on carbon fiber and POSS surfaces. The related chemical reaction known as "thiol-ene" click chemistry is more feasible for the carbon fiber and POSS grafting. Thiol-ene click reactions occur between a thiol ($-$SH) and alkene (carbon–carbon double bond). The reaction can also be initiated by a variety of methods, with simple and quick free radical reactions making them highly efficient to produce. Through a series of reactions, it is possible to thiolate the surface of the carbon fiber, to facilitate one of the required functional groups ($-$SH), and the commercially available octavinyl-POSS will act as the other functional group. The simplified reaction is shown below in Figure 2.1. Kuttner and co-workers, utilized this same thiol-ene photochemistry reaction to link thiolated glass fibers to polystyrene of different lengths and densities [47, 48]. This work highlights the feasibility of thiol-ene click chemistry in the modification of fiber surfaces.

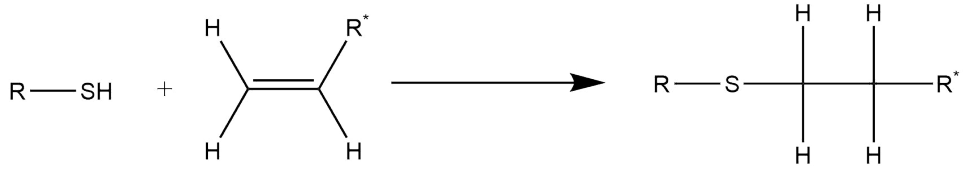

Figure 2.1: Simplified Thiol-ene Click Reaction.

This research improves the interfacial properties of carbon fiber polymer matrix mate-

rials by creating a controlled and uniform coating of POSS based materials. Utilizing the highly efficient click chemistry, to achieve a more complete coverage of the fiber, will limit localized points of failure. A relatively new less aggressive oxidation treatment in combination with the mild reaction conditions of click chemistry preserves the fiber strength during the grafting reaction. In this manner, the current study overcomes the two current limitations in the coating of carbon fibers using POSS. The treatments are fully characterized by XPS and SEM. The effects of these treatments on the mechanical and interfacial properties are examined using single-fiber tensile and single-fiber fragmentation testing, respectively.

2.1 Materials and methodology

All chemicals were used as received unless otherwise stated. Carbon fibers used were HexTow IM-7 (12K, tensile strength 5.65 GPa, diameter 5.2 µm, density 1.78 g/cm^3), and purchased from HEXCEL (HEXCEL, Stamford, Connecticut). Octavinyl-POSS was purchased from Hybrid Plastics (Hybrid Plastics, Hattiesburg, Mississippi). Dimethylformamide (DMF), Sulfuric acid, nitric acid, 6-mercapto-hexanol, p-Toluenesulfonic acid (p-TSA) and 2,2-Dimethoxy-2-phenylacetophenone were supplied by Fisher Chemicals (Fisher Scientific, Pittsburgh, Pennsylvania). Potassium persulfate ($K_2S_2O_8$) and silver nitrate ($AgNO_3$) were purchased from Sigma-Aldrich (MilliporeSigma, St. Louis, Missouri). Tetrahydrofuran (THF) was supplied by EMD Chemicals (EMD Chemicals, Burlington, Massachusetts) and the UV hand lamp was purchased through VWR (VWR, Radnor, Pennsylvania). EPON 862 and EPIKURE 3274 were supplied by Miller-Stephenson (Miller-Stephenson, Danbury, Connecticut).

2.1.1 Coating of carbon fibers with POSS via esterification

The reaction between POSS and the carbon fiber surface used in approach one required the chemical preparation of both the carbon fiber surface and octavinyl-POSS. To enable

POSS to both chemically bind to the surface of a carbon fiber and play an important role in enhancing mechanical strength of carbon fiber, the thiol-ene click chemistry was used to partial hydroxylate commercially available Octavinyl-POSS. In this reaction, shown below in Figure 2.2, 632.3 mg (1.0 mmol) of vinyl-POSS (**1**), 537 mg (4.0 mmol) of 6-mercaptohexanol (**2**) and 51.26 mg (0.2 mmol) of the catalyst DMPA (**3**) were added to a 10 mL round-bottom flask containing 5 mL of toluene. This reaction mixture was placed under a UV lamp (365nm) with stirring and continued the UV-assisted thiol-ene click chemistry at room temperature for 5 hours. The product (**4**) was separated from unreacted components and toluene solvent by vacuum distillation, and the isolated product was vacuum dried to remove traces of toluene solvent.

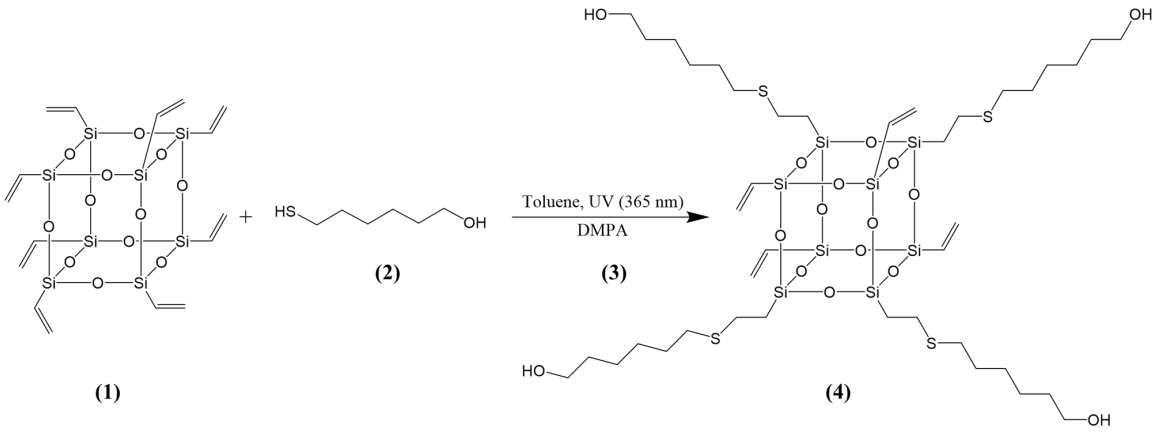

Figure 2.2: Synthesis of Vinyl-Hydroxyl-POSS using "Thiol-ene" Chemistry.

To functionalize the carbon fibers, an acid catalyzed esterification reaction was done between the hydroxyl functional POSS (**4**) and carboxylic acid functional groups along the carbon fiber surface. The as-received carbon fibers were first unsized by soaking them in acetone for 24 hours, this removes any manufacturers sizing treatment. The unsized fibers (**5**) (500 mg) were then oxidized using a 3:1 sulfuric acid and nitric acid (68-70%) solution at 60°C for 60 minutes with continuous sonication. Subsequently, the fibers were repeatedly rinsed with DI water to obtain neutralized fiber. This oxidation process increases the number of carboxylic acid groups on the surface of the carbon fiber and allows for

the desired surface modification (**6**). For the functionalization of this carboxylated carbon fibers (**6**) with hydroxyl functional POSS (**4**), an acid catalyzed esterification reaction was carried out. In this reaction, 1.10 g of Vinyl-Hydroxyl-POSS product (**4**, 0.94 mmol) and 300 mg of the oxidized carbon fibers (**6**) were added to a round-bottom flask containing 50 mL of DMF. The flask was placed in an oil bath with stirring and catalytic amounts of sulfuric acid was added and left to react at 60°C for 24 hours. The POSS functionalized carbon fibers (**7**) were rinsed with fresh DMF to remove unreacted octavinyl-POSS and the fibers were dried at 100°C for 2 hours. The reaction is shown in Figure 2.3.

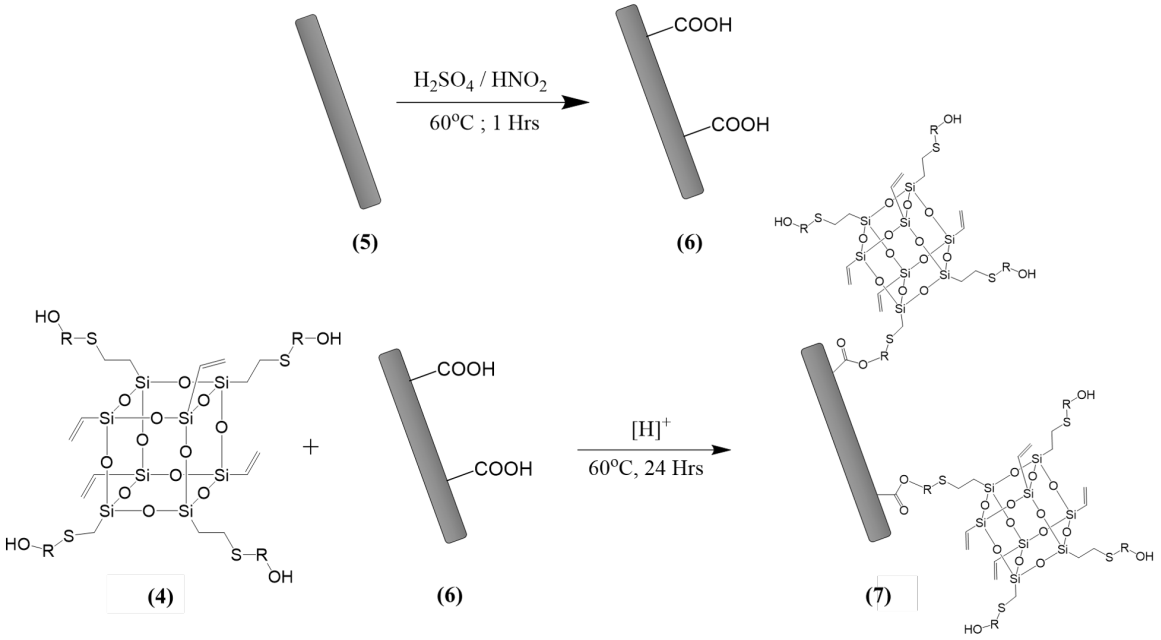

Figure 2.3: Synthesis of POSS coated carbon fibers using esterification reaction, noted as approach one.

2.1.2 Coating of carbon fibers with POSS using thiol-ene chemistry

The reaction between POSS and the carbon fiber surface used in approach two required the chemical preparation of only the carbon fiber surface. In this approach the octavinyl-POSS was used as-received. The preparation of the carbon fiber surface occurred through the following series of reactions. The as-received carbon fibers (500 mg) were unsized by placing them in acetone for 24 hours. This removed any pre-existing chemical sizing treatment.

The unsized carbon fibers (**5**) were oxidized using a mixture of 0.1M $K_2S_2O_8$ and 0.01M $AgNO_3$ for 60 minutes at 70°C with sonication. The oxidized fibers (**8**) (CF-COOH), were removed from the reaction mixture and washed with DI water until neutralized and then dried at 100°C for 24 hours. The CF-COOH fibers (**8**) were added to a round bottom flask containing 6-mercapto-hexanol (1 g) in toluene (100 ml) and catalytic amounts of p-Toluenesulfonic acid (p-TSA). This is left to react for 24 h at 60°C. The resulting (CF-SH) fibers (**9**) were rinsed with fresh toluene and dried at 100°C for 24 hours. This series of chemical reactions is illustrated below in Figure 2.4.

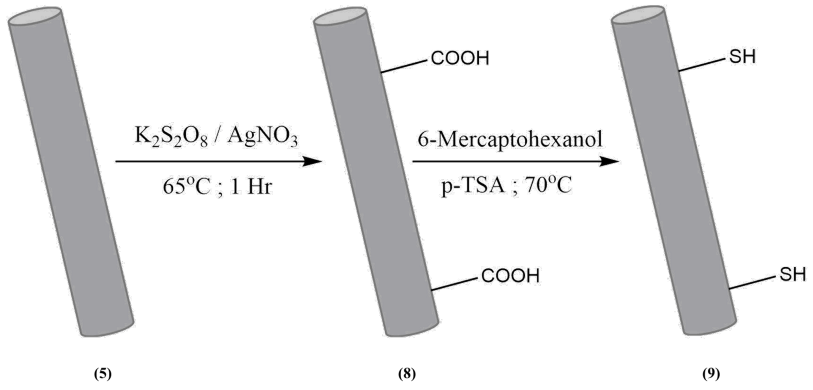

Figure 2.4: Oxidation and thiolation of carbon fibers.

Octavinyl POSS (**10**) (2 g) and the CF-SH fibers (**9**) were added to a round bottom flask containing 100 ml of DMF at 50°C for 2 hours. The reaction was initiated using 2,2-Dimethoxy-2-phenylacetophenone (DMPA) and a UV light with an intensity of 365 nm. This creates thiol radicals that react with the double bonds of octavinyl-POSS, clicking the POSS to the fiber surface. The resulting (CF-POSS) (**11**) fibers were rinsed with THF to remove excess POSS material and dried at 100°C for 24 hours. The chemical reaction and the final carbon fiber clicked-POSS are shown below in Figure 2.5.

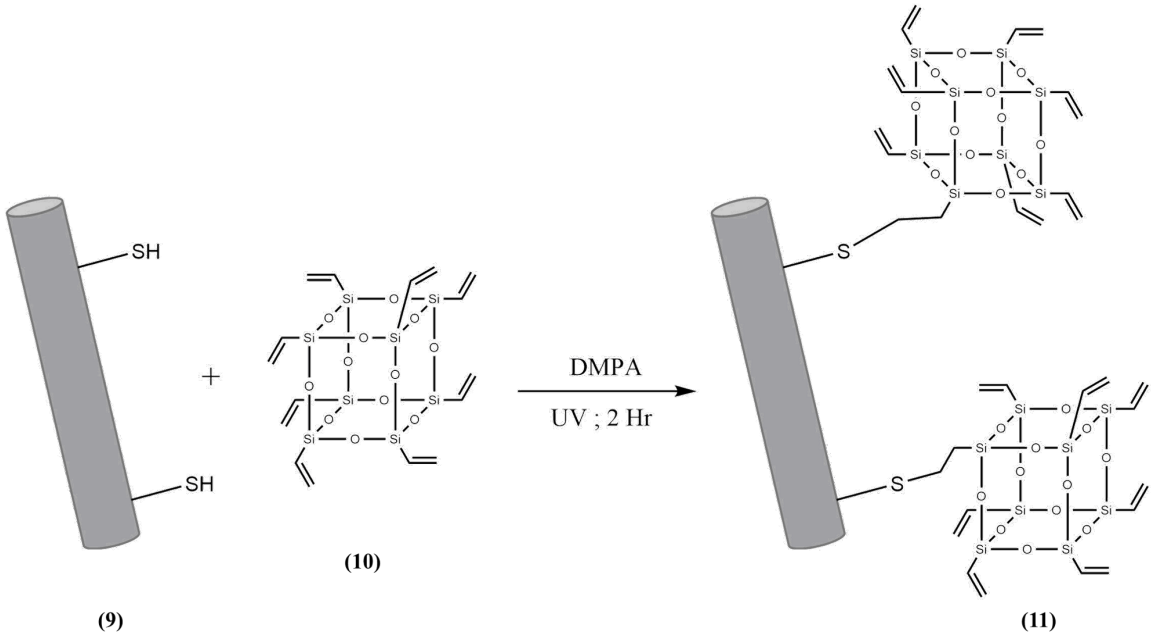

Figure 2.5: Reaction between thiolated fibers and octavinyl-POSS using thiol-ene chemistry, noted as approach two.

2.1.3 Characterization techniques

Nuclear Magnetic Resonance (NMR, Bruker DPX-300 NMR Spectrometer) and Fourier Transform Infrared (FTIR, Perkin Elmer Spectrum Two) were utilized to characterize the hydroxylated POSS used for the esterification reaction in approach one. X-ray photoelectron spectroscopy (XPS, PHI VersaProbe) and scanning electron microscope/Energy Dispersive X-Ray Spectroscopy (SEM/EDS, Hitachi S-4800 Field Emission Scanning Electron Microscope) was utilized to analyze the carbon fibers surface chemical composition and topographical changes throughout the chemical modification process.

Tensile strength of a single fiber filament was performed on a universal testing machine (5567, Instron Corporation, Norwood, Massachusetts) according to ASTM C1557-06. A hole was cut in the middle of a paper testing tab and the monofilament was separated from the fiber tow using masking tape under magnification. The monofiliament was secured on one end of the tab and aligned in the center then adhered to the other end of the tab using

masking tape, then super glue was used to further adhere the fiber to the ends of the paper tab. The tab was placed in the grips of the testing machine and the sides of the tab were cut so that only the fiber would undergo loading. A gauge length (l_f) of 40.9 mm and a cross-head speed of 1 mm/min loading rate was used for all fiber samples. The maximum load at which the fiber failed was recorded and was used to determine the tensile strength using the equation 1,

$$\sigma_f = P_f/A \tag{1}$$

where σ_f is the tensile strength of the fiber, P_f is the load at which the fiber fails, and A is the cross-sectional area calculated as $A = \pi d^2/4$ in terms of the fiber diameter, d. The fiber diameter was determined using scanning electron microscopy (SEM).

There is expected to be a great deal of variation in the tensile strengths among the fibers.This variation is a result processing, the fiber microstructure and flaw distribution along the length of the fiber [49]. Weibull probability distribution is often used to represent this variation in tensile strength. Along with this, the Weibull modulus, m, is used in the calculation of the interfacial shear strength. To determine the Weibull modulus, the tensile data collected before is used to generate a Weibull plot, utilizing the common two–parameter Weibull distribution below in equation 2 and rearranged into equation 3:

$$p(\sigma) = 1 - \exp\left(-\frac{l_c}{l_f}\left(\frac{\sigma_c}{\sigma_f}\right)^m\right) \tag{2}$$

$$\ln\left(\ln\left(\frac{1}{1-p(\sigma)}\right)\right) - \ln\left(\frac{l_c}{l_f}\right) = m(\ln\sigma_c - \ln\sigma_f) \tag{3}$$

Where $p(\sigma)$ is the probability of failure. l_c is the critical fiber fragmentation length, which is determined during the single–fiber fragmentation tests and l_f is the gauge length. σ_f and σ_c are the fiber strengths at the gauge length and at the critical fiber length, respectively and m is the Weibull modulus. Utilizing a consistent gauge length, equation 3

becomes equation 4 below:

$$\ln\left(\ln\left(\frac{1}{1-p(\sigma)}\right)\right) = m(\ln\sigma_c - \ln\sigma_f) \tag{4}$$

The Weibull modulus, m is derived from a plot of $\ln\sigma_f$ versus $\ln\left(\ln\left(\frac{1}{1-p(\sigma)}\right)\right)$ where $p(\sigma)$ is equation 5

$$p(\sigma) = \frac{i}{N+1} \tag{5}$$

where i is the rank of each data point and N is the total number of samples.

The interfacial shear strength (IFSS) was determined using the single–fiber fragmentation test (SFFT). The single fiber fragmentation test was developed from the Kelly–Tyson simple force balance formula below in equation 6 for a fiber under static loading conditions as demonstrated in Figure 2.6.

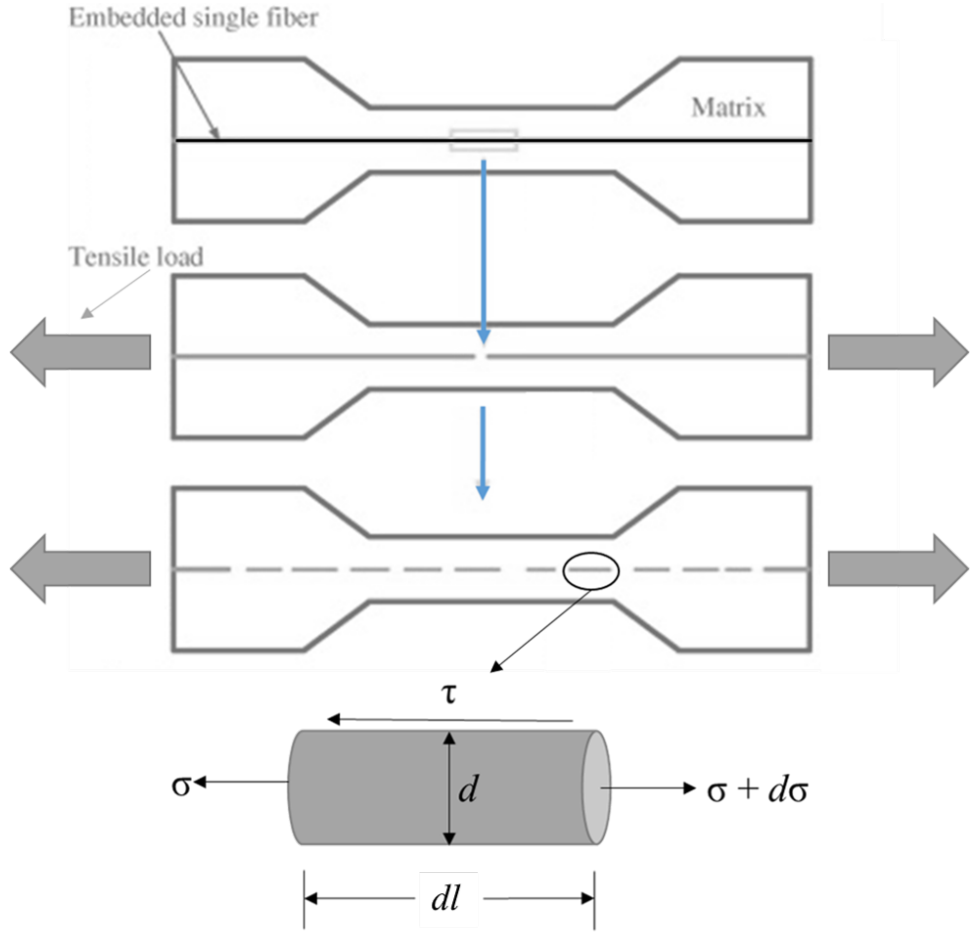

Figure 2.6: Forces on a fiber under static loading conditions.

The fiber is held under static loading, we can sum the forces in the x-direction and derive the below equation 6:

$$\sum F_x = (\sigma + \mathrm{d}\sigma)\frac{\pi d^2}{4} - \sigma\frac{\pi d^2}{4} - \tau(\pi d)\mathrm{d}l = 0 \tag{6}$$

This equation can be simplified and integrated from no load (σ_0) to a critical load which breaks the fiber (σ_c) and over the length of the fiber (l) in equations 7 and equation 8, respectively.

$$\frac{\mathrm{d}\sigma}{\mathrm{d}l} = \frac{4}{d}\tau \tag{7}$$

$$\int_{\sigma_0}^{\sigma_c} \mathrm{d}\sigma = \frac{4}{d}\int_0^l \tau \mathrm{d}x \tag{8}$$

Assuming that the fiber will break at $l/2$ and solve for τ the interfacial shear strength in equation 9

$$\tau = \frac{\sigma_c d}{2l_c} \tag{9}$$

where τ is the interfacial shear strength, σ_c is the fiber strength at the critical fiber length, l_c is the critical fiber fragment length and d is the fiber diameter [50, 51]. The critical fiber length is the length at which the fragments are too short for sufficient load to be transferred onto them to cause additional failure, also called the saturation point. At this point the lengths of the fragments reflect the interfacial shear strength of the fiber–matrix interface. Determination of this point is done via the single fiber fragmentation test.

To prepare samples for the single fiber fragmentation test a single fiber was aligned along the center of a dog bone shaped mold, shown in Figure 2.7. The fiber was secured at both ends to prevent movement during the curing process. Appropriate amounts of EPON 862 and the curing agent EPIKURE 3274 were mixed and degassed then poured into the dog bone shaped mold. This was cured and the coupon was removed from the mold and polished for better visualization of the fiber.

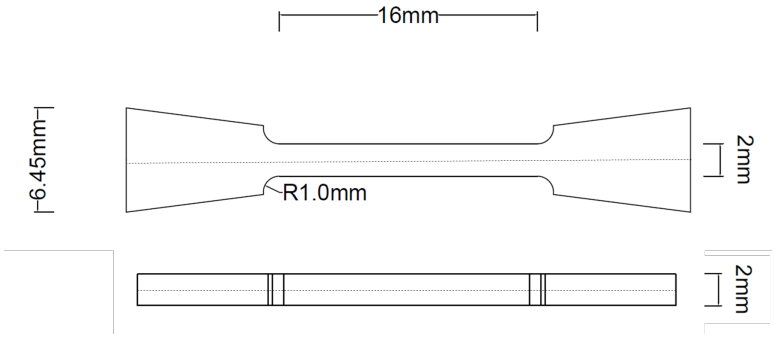

Figure 2.7: Specimen dimensions for the dog bone shaped coupon.

A tensile testing setup was designed to facilitate the requirements of the single fiber fragmentation test. Two grips were machined to hold the specimen and prevent slippage

properly, one of these grips was attached to a motorized linear slide (Oriental Motors, Taito–Ku, Tokyo, Japan), and the other was mounted to a load cell (OMEGA Engineering, Norwalk, Connecticut, USA) to monitor the load during testing. The linear slide and load cell were secured to a table and positioned under a Nikon optical microscope fitted with a camera. The complete setup is shown in Figure 2.8. During the testing process, as the single fiber coupon undergoes tensile loading, the load is transferred to the fiber in the form of shear stress across the fiber–matrix interface. These shear stresses generate a tensile stress in the fiber. As the applied load is increased, the tensile stresses in the fiber cause it to break into shorter and shorter fragments. When no further load can be transferred to the fiber, the breaks stop occurring and saturation is reached. This is when the fragments are too short for sufficient load to be transferred to the fiber. The breaks in the fibers are examined using an optical microscope and monitored in real-time to ensure saturation is reached.

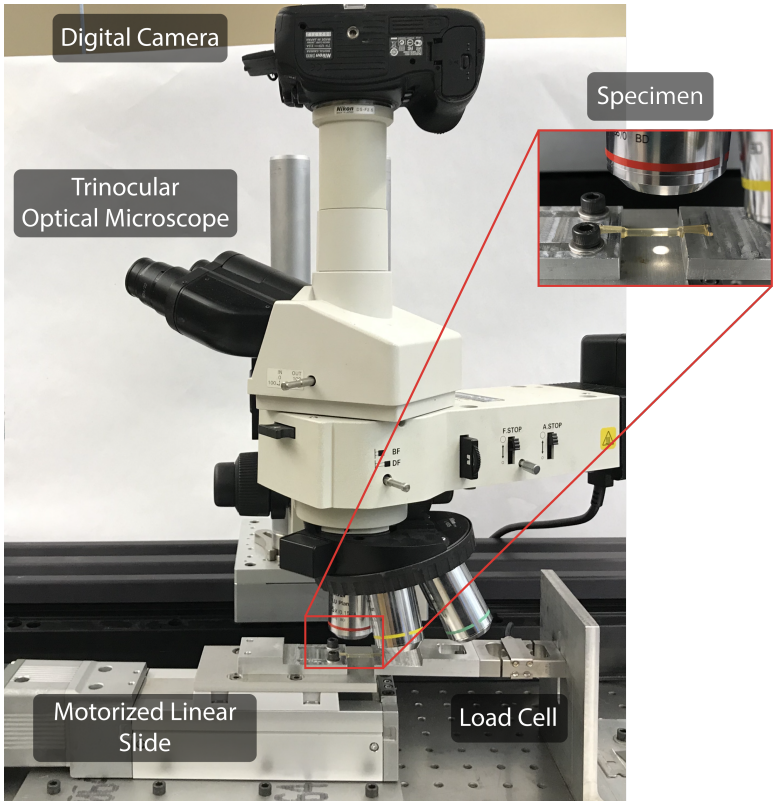

Figure 2.8: Single fiber fragmentation testing setup.

The fiber is monitored as the load is increased until no more breaks are observed and multiple images captured. Using a calibration grid, the distance between these breaks can be determined and averaged to find $< l >$. The critical fiber length is calculated from the average fiber length as $l_c = \frac{4}{3} < l >$. The fiber strength at the critical fiber length is calculated using the tensile strength determined earlier, with the gauge length of 40.9mm (l_f) and Weibull modulus (m).

2.2 Results and Discussion

2.2.1 Characterization of modified POSS

The vinyl-POSS was modified using thiol-ene chemistry, a class of highly efficient and simple chemistry referred to as a thiol-ene click reaction. The reaction is initiated using 2,2-Dimethoxy-2-phenylacetophenone (DMPA) and a UV light with an intensity of 365 nm. The photoinitiated reaction creates thiol radicals that react with the double bonds of the octavinyl-POSS, clicking the two molecules in a very neat reaction. In order to obtain partially hydroxylated vinyl POSS, we have used four equivalent of 6-mercaptohexanol to one equivalent of vinyl-POSS molecules and the reaction was continued for 5 hours. To characterize this reaction, Fourier-transform infrared spectroscopy (FTIR) was utilized and is shown in Figure 2.9. The spectra shows the silicon oxygen bonds of the POSS inorganic cage (1100 cm^{-1}), unreacted double bonds (3030 cm^{-1}) and the terminal hydroxyl group from the clicked 6-mercaptohexanol (3390 cm^{-1}), indicative of the formation of the desired product. This set of reactive groups will allow for the bonding of POSS to the surface of carbon fibers utilizing esterification, and also allow for further layers of POSS to be added to the interphase region through more thiol-ene reactions.

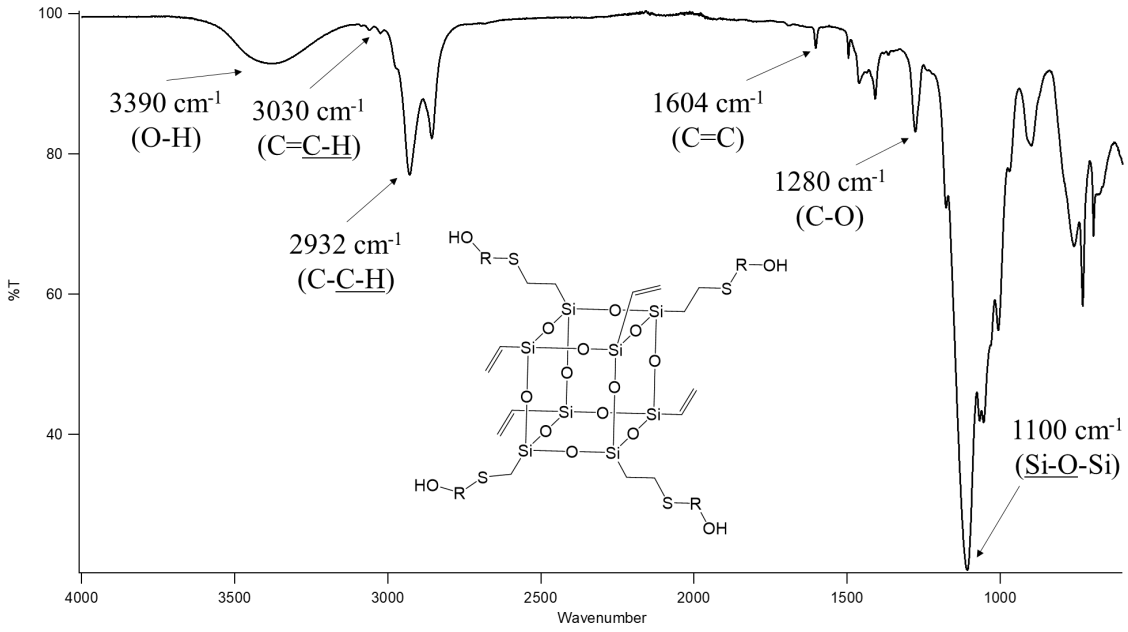

Figure 2.9: FTIR Spectra of synthesized vinyl-hydroxyl-POSS.

To further characterize the synthesized vinyl-hydroxyl-POSS, Nuclear Magnetic Resonance (NMR) was used to confirm the structure. The Octa-vinyl POSS was dissolved in $CDCl_3$, while the 6-mercaptohexanol and modified POSS material (**4**) was dissolved in DMSO-D_6, the spectra are shown in Figure 2.10. The presence of the characteristic peak at 0.954 ppm confirmed the successful thiol-ene click reaction and indicative of product formation. In addition, the presence of weak signal at 5.94 ppm indicated the presence of alkenes, which further confirmed for the partial hydroxylation of vinyl-POSS. Other characteristic peaks were present in the product: **F** (4.33 ppm) representing the presence of primary hydroxyl groups, which can be utilized to conjugate carbon fiber. As mentioned earlier, the peak at **G/H** (5.94/6.09 ppm) is indicative of the remaining alkene functional group, which will be important for subsequent click reactions to build multiple POSS layers for future work. The other peaks in the spectra can all be accounted for within the structure and represent the protons within the alkane chain, their position is based upon the distance from the hydroxyl and sulfur groups. These results indicated for the successful synthesis and isolation of pure vinyl-hydroxyl-POSS, the spectra does not show any unexpected

peaks.

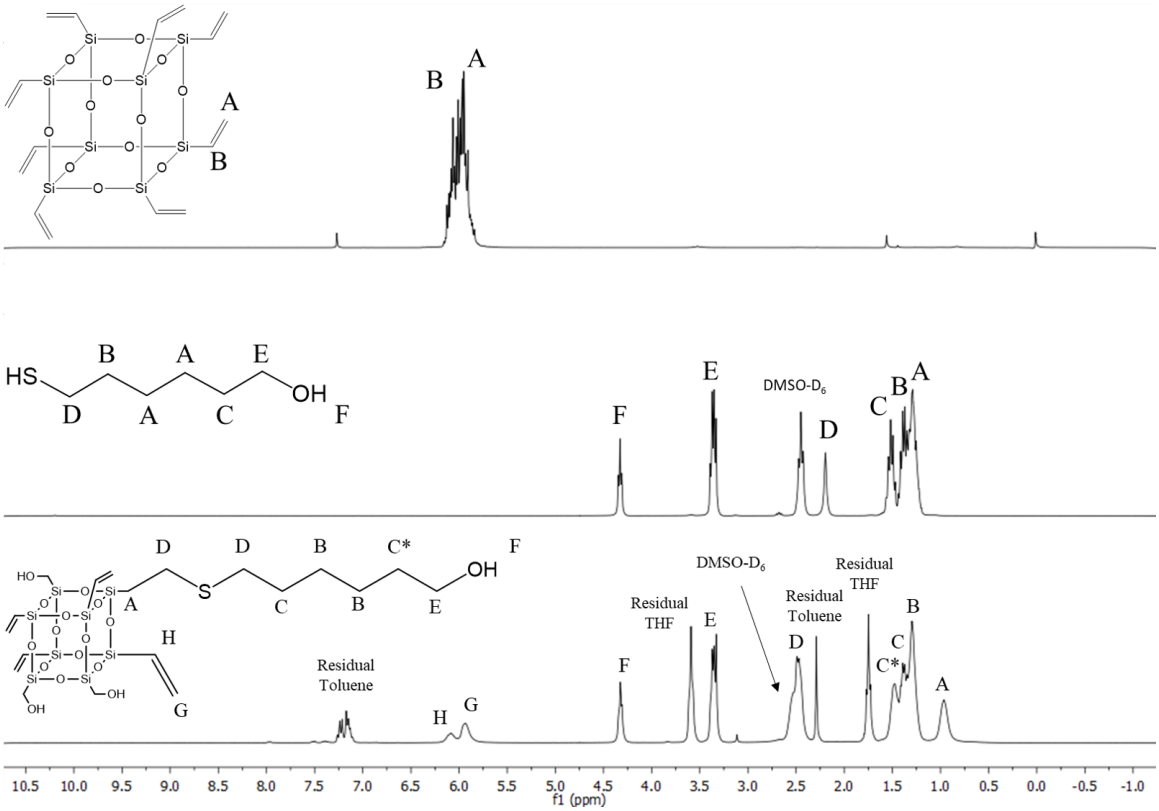

Figure 2.10: ^{1}H NMR Spectra of the vinyl-hydroxyl-POSS coated carbon fibers.

2.2.2 CF surface chemical composition and topographical analysis using XPS and SEM

The as-received IM-7 carbon fibers were left in acetone for 24 hours, to remove any manufacturer sizing treatments. These unsized fibers were used as the starting point for both approaches. XPS was used to characterize the changes in chemical composition of the fiber surface. In the first approach, acid oxidation was used followed by ester reaction with the modified POSS and the results are shown below in Table 2.1. It can be seen that the oxidized fibers had an increase in the oxygen content from 6.2% to 16.7%, a 170% increase. The reaction between the hydroxyl groups on the modified POSS and the carboxylic acid groups present on the carbon fiber surface was done using catalytic amounts of sulfuric acid. The chemical composition shows a silicon content of 4.2% and a further

increase in the oxygen content to 20.4% due to the silicon-oxygen cage of the POSS material. These results indicate successful chemical reactions of both the oxidation and POSS coating through the reaction between hydroxyl and carboxylic acid.

Table 2.1: Surface composition analysis of carbon fibers using approach one

Samples	Elemental content (%)				
	C	O	Si	S	O/C
As-received	80.7	16.3	3.0	-	0.20
Unsized	90.3	6.2	1.1	-	0.07
Oxidized CF	79.7	16.7	2.1	-	0.21
POSS-Coated CF	73.1	20.4	4.2	0.1	0.27

The compositional changes of the carbon fibers coated using methods 2 is shown in Table 2.2. The oxidation of the carbon fibers using the aqueous solution of $K_2S_2O_8$ and $AgNO_3$ showed a significant increase in the oxygen content from 6.2% to 15.4%. This method of oxidation, although not as aggressive as acid oxidation, produced very similar oxidation levels. The oxidized fibers were then reacted with 6-mercaptohexanol to yield thiol-functionalized carbon fibers. The XPS analysis shows the resulting increase in sulfur content, 12.3%. These thiol groups expressed on the surface of the carbon fiber were then reacted with the double bonds of the octavinyl-POSS utilizing thiol-ene chemistry. These fibers were again analyzed using XPS and resulted in an increase in both the silicon and oxygen elemental percentages. This is a result of the silicon-oxygen cage of the POSS material. The surface chemical analysis of the modified fibers demonstrates the successful use of thiol-ene chemistry as a method for grafting POSS to the surface of carbon fibers.

Table 2.2: Surface composition analysis of carbon fibers using approach two

Samples	Elemental content (%)				
	C	O	Si	S	O/C
As-received	80.7	16.3	3.0	-	0.20
Unsized	90.3	6.2	-	-	0.07
Oxidized CF	80.7	15.4	-	-	0.19
Thiolated CF	74.4	12.8	-	12.3	0.17
POSS-Coated CF	66.5	20.6	3.8	4.6	0.31

The fiber surface was visually analyzed using SEM and the final POSS coated fibers were analyzed using the EDS function of the SEM. The IM-7 as-received carbon fiber surface and the unsized fibers are shown in Figure 2.14. The as-received fibers show little surface features, most likely due to a sizing treatment used by Hexcel. The fibers were unsized using acetone, and by stripping the fiber surface, the sizing material is removed and the bare fibers are exposed.

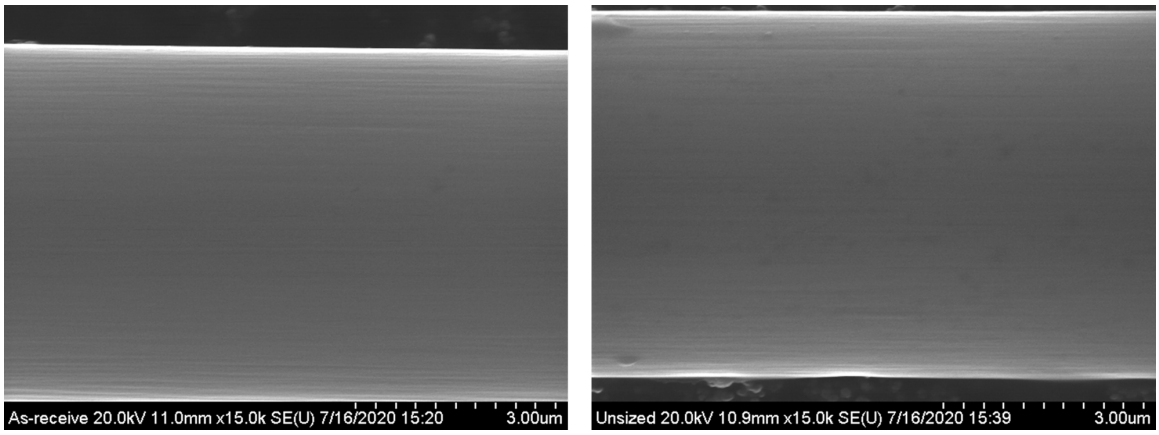

Figure 2.11: As-received IM-7 carbon fibers (left) and unsized carbon fibers (right).

The unsized fibers were then oxidized utilizing two different methods, the common method of H_2SO_4/HNO_3 and a less aggressive method utilizing $AgNO_3/K_2S_2O_8$. The

results of these two treatments on the surface of the fiber are shown in Figure 3.1. On the left the common H_2SO_4/HNO_3 method shows some blistering of the fiber surface and some flaking of the fiber surface. The method utilizing $AgNO_3/K_2S_2O_8$ shows no blistering or flaking of the surface, and the surface is relatively unchanged visually when compared to the unsized fibers.

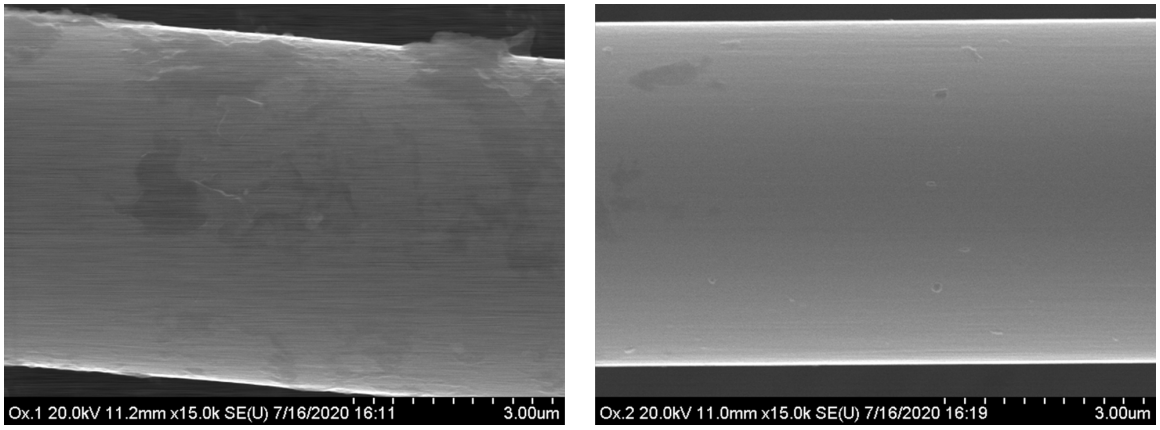

Figure 2.12: Effect of H_2SO_4/HNO_3 oxidation on the carbon fiber surface (left) and effect of $AgNO_3/K_2S_2O_8$ on the carbon fiber surface (right).

Finally, the fiber surfaces after treatment with both POSS coating treatments are shown below. Image 2.13a shows the results of POSS-coating using esterification reaction between the modified POSS and oxidized carbon fiber. The image shows a large region of bare fiber and other areas with a thick POSS-coating. This nonuniform coating on the fiber surface could result in poor interaction with the matrix material and cause a weaker overall composite. On the right, thiol-ene chemistry was used to react the as-received octavinyl-POSS material with the thiolated carbon fibers. The results of the thiol-ene reaction shows a very uniform coating of POSS. The coating appears to almost fully coat the surface while avoiding agglomeration of excess POSS. This uniform coating should result in more uniform properties along the fiber–matrix interface. The presence of POSS was confirmed using EDS, areas containing silicon are highlighted in green. The upper images representing the first attempt at POSS-coating show large areas of bare fiber, not containing the POSS-coating. However, the lower images, which utilized thiol-ene click chemistry as the

method of coating, show a very uniform distribution of silicon containing POSS.

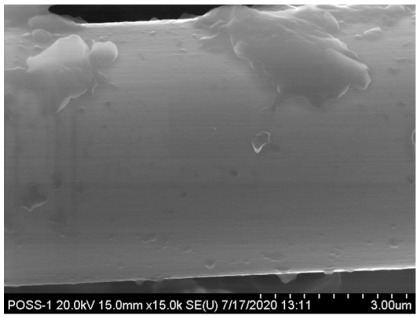

(a) SEM image of POSS coating using approach one

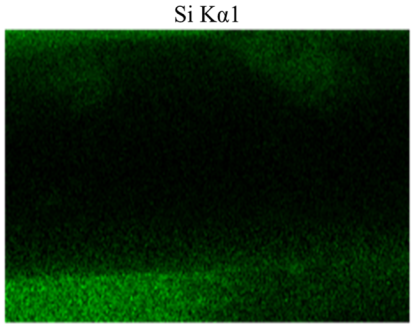

(b) Approach one POSS coating examined using EDS, the green represents areas containing silicon

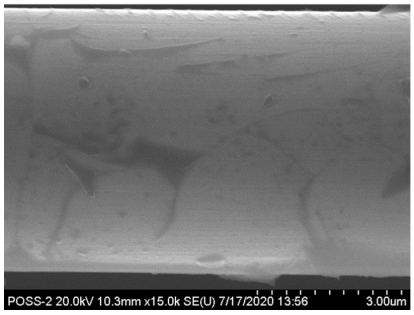

(c) SEM image of POSS coating using approach two, thiol-ene click chemistry

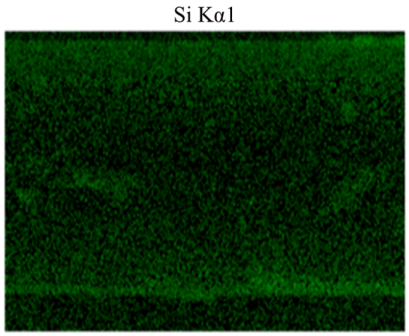

(d) Approach two POSS coating examined using EDS, the green represents areas containing silicon

Figure 2.13: SEM and EDS images of POSS approach one and two, with the presence of silicon highlighted in green in the EDS images

2.2.3 Mechanical characterization of carbon fiber treatments

2.2.3.1 Single–fiber tensile testing

The fiber strength was obtained using single–fiber tensile testing. The results of the single fiber tensile tests were then used in the determination of the Weibull modulus. The number of tensile tests used in the determination of the Weibull modulus was 10 samples from each fiber conditions. This number of tests means that there could be discrepancy in the accuracy of the Weibull modulus. Swolfs *et al.* reported that to obtain less than 10% variation several hundred fibers would have to be tested [52]. However it is not uncommon for researchers to

use samples sizes in the range of 5-60 fiber samples tested [53–55]. While it is established that more tests results in a more accurate Weibull modulus, comparing the experimental data to a best–fit line and achieving relatively high coefficients (R^2) has been used to gauge reliability in the Weibull data [55]. The mean tensile strengths, Weibull modulus and R^2 values are shown below in Table 2.3. The results show that the first approach in treating the carbon fibers and the oxidation method used caused a substantial decrease in the fiber strength. The aggressive acid oxidation used in the first method resulted in much greater variability in the fiber strength causing a sharp decrease in the Weibull modulus. The second approach which utilized a much less aggressive oxidation method did not exhibit a loss in fiber tensile strength. In both approaches, the fibers saw an increase in tensile strength after reacting with POSS. It is believed that POSS helps mitigate the effects of surface flaws along the fiber, resulting in improved tensile properties. All samples showed relatively high coefficients (R^2) and demonstrated reasonable conformity between the best-fit line and experimental Weibull modulus data.

Table 2.3: Results of single–fiber tensile testing

Fiber Condition	Mean Tensile Strength (GPa)	Weibull Modulus	R^2
As-Received	3.9 ± 0.7	5.5	0.85
Unsized	3.8 ± 0.4	8.3	0.88
Oxidized (H_2SO_4/HNO_3)	1.4 ± 0.6	2.9	0.97
Oxidized ($AgNO_3$/$K_2S_2O_8$)	3.9 ± 0.5	6.1	0.90
Approach 1 POSS-Coating	2.9 ± 0.4	5.5	0.99
Approach 2 POSS-Coating	4.4 ± 0.8	5.2	0.93

2.2.3.2 Single–fiber fragmentation test

The single fiber dog bone shaped coupons were subjected to loading intervals of 15 seconds or approximately 25N, at a loading rate of 0.01mm/second. The test was paused for 60 sec-

onds after each 25N interval and the length of the fiber was evaluated under magnification and breaks could be recorded. This cycle was repeated until saturation occurred, at this point fiber breaks could be easily seen under microscope and images were captured and analyzed. A typical loading plot and images of fiber breaks (breaks circled to emphasize) is shown below in Figure 2.14. The distance between these fiber breaks was determined using a calibration grid and the software "ImageJ" [56].

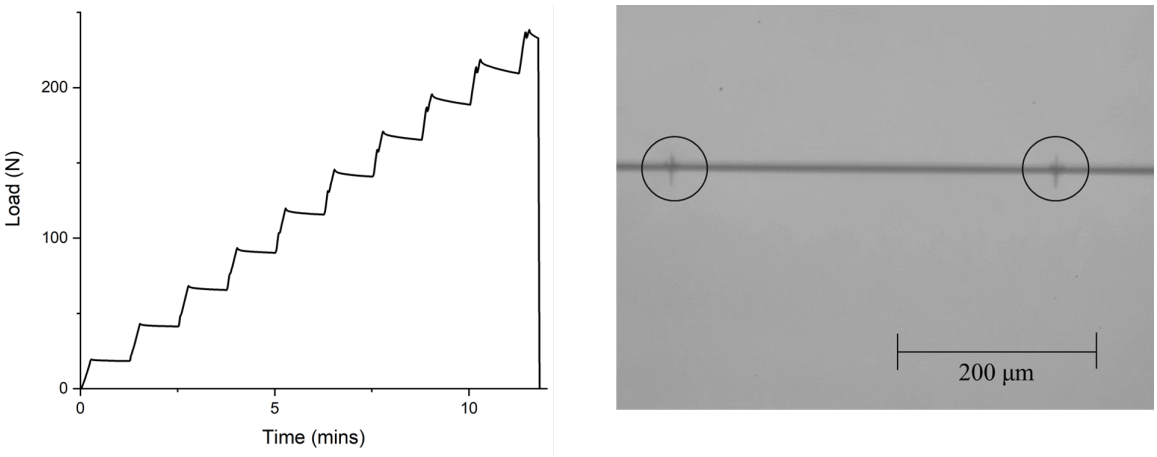

Figure 2.14: Typical loading data for single fiber fragmentation test and image of the fiber breaks (breaks circled) as the specimen is under load.

Multiple coupons were prepared for each of the different fiber conditions, as-is, unsized, oxidized (H_2SO_4/HNO_3), oxidized ($AgNO_3/K_2S_2O_8$), POSS-coating using approach one and finally POSS-coating using approach two utilizing thiol-ene chemistry. The specimens of each treatment were tested to a point of fiber break saturation. The fiber lengths are recorded, and the critical fiber length l_c determined for each test. The final l_c values were averaged to achieve a final critical fragmentation length, compiled in Table 2.4.

Generally speaking, a greater adhesion between fiber and matrix results in a shorter fiber fragment length. The unsized fibers showed a significantly larger fragmentation length compared to the as-received fibers. This is due to the inert and smooth surface that is typical of bare carbon fibers. As the unsized fibers were oxidized in both approaches it can be observed that the fiber fragment lengths were similar to the as-received carbon fibers.

The oxidation that uses H_2SO_4/HNO_3 has a much shorter fragmentation length than the oxidation using ($AgNO_3/K_2S_2O_8$). However, due to the decrease in fiber strength the interfacial shear strength is actually higher in the oxidation method using ($AgNO_3/K_2S_2O_8$) . The POSS coated fibers result in a further decrease in fragment length which means the adhesion between the fibers and the matrix is better. In the first approach, fiber fragmentation lengths decreased 24% compared to the as-received fibers. The second approach, fiber fragmentation lengths decreased 27% as compared to the as-received fibers indicating a greater increase in the interfacial shear strength. The fiber fragmentation length cannot be used to directly measure the adhesion between the fiber and matrix. However, it is used in the calculation, of the interfacial shear strength using the force balance equation, $\tau = \frac{\sigma_c d}{2l_c}$. The last variable to be determined is the fiber strength at the critical fiber fragment length.

The critical fiber length and the Weibull modulus which was calculated earlier are used to calculate the fiber strength at the critical fiber length, σ_c. The IFSS was found for all of the different fiber conditions and is also listed in Table 2.4. The results of these tests show that the as-received and oxidized fibers had very similar interfacial shear strengths. The first approach to POSS coating of carbon fibers showed little difference to the as-received or the oxidized. Although the fiber fragmentation length of the first approach to POSS coating were smaller than either of the oxidized or the as-received fibers, the interfacial shear strength was not improved. This is due to the significant decrease in the fiber tensile strength, which negatively impacts the interfacial shear strength. The second approach used in coating the carbon fibers with POSS, however, utilized a much less aggressive oxidative treatment. This maintained the fiber strength. The critical fiber length obtained from this approach is also much shorter. The result of both the maintaining of the fiber strength and the reduction in the critical fiber length resulted in an 71% increase in interfacial shear strength compared to as-received fibers.

Table 2.4: Fragmentation length and interfacial shear strength (IFSS) for the various fiber conditions.

Fiber Condition	Critical Fiber Length (μm)	IFSS (MPa)
As-Received	550 ± 119	41.0
Unsized	660 ± 141	25.1
Oxidized (H_2SO_4/HNO_3)	462 ± 94	35.6
Oxidized ($AgNO_3/K_2S_2O_8$)	557 ± 84	35.2
Approach 1 POSS-Coating	443 ± 63	38.4
Approach 2 POSS-Coating	400 ± 51	70.1

2.3 Conclusion

This work examined the use of click chemistry as a mechanism for better and more thorough chemical grafting of polyhedral oligomeric silsesquioxane to improve the interfacial properties. This method of POSS-coating (approach two) was then compared to literature and a proposed alternative method (approach one). Approach one used a methodology that differed only slightly from common literature approaches and was used to compare approaches and verify our testing setup. The chemical process of the modified POSS used in approach one was successfully characterized using NMR and FT-IR. The fibers from both approaches were fully characterized using x-ray photoelectron spectroscopy, which monitored the surface composition. The results were as expected, confirming our proposed chemical modifications of the fibers. The surface changes were characterized using scanning electron microscope and images show how the fiber surface changes as a result of chemical treatment and show the results of the two different POSS treatments on surface coverage and uniformity.

The mechanical properties of the carbon fibers were characterized using single fiber tensile tests. The results showed that the more aggressive oxidation method used in the

first approach had a detrimental effect on fiber strength. The second approach, however, utilized a less common and less aggressive oxidation treatment, as a result no change in fiber strength was recorded. Lastly, the interfacial properties were characterized using single fiber fragmentation test. This is considered one of the best methods for determining the micro-mechanical properties of composite materials. The tests were conducted and analyzed for each of the fiber conditions. The first approach showed almost no change in the interfacial shear strength. This can be attributed to the decrease in fiber strength, and lower yielding esterification reaction that was used as the coating method. The secondary approach showed an interfacial shear strength improvement of 71% as compared to the IM7 carbon fibers. This increase is much greater than values found in literature that follow a similar approach to our first POSS treatment.This implies that the use of thiol-ene chemistry and mild oxidation provide increases in fiber–matrix interaction that far surpass other methods to date.

CHAPTER III

Multilayer POSS treatment to control interface compliance

3.1 Introduction

It has been long understood that the properties of the interphase region play an important role in the mechanical stiffness, strength, and toughness of fiber-reinforced polymer matrix composites [57, 58]. In general, a well-bonded fiber-matrix interface coupled with a stiff interphase region leads to higher overall composite stiffness and strength. This is because of enhanced load transfer mechanism. However, the role of the interphase region in governing the strength and toughness of composites is complex and often involves competing mechanisms. For example, Eskandari *et al.* showed that a stiffer interphase leads to greater compressive strength in fiber-reinforced composites [16]. This was confirmed by Needleman *et al.* for the case of a carbon nanotube reinforced polymer matrix composite [17]. It was shown that an interphase with higher elastic modulus and yield strength led to increased composite stiffness and strength. However, Eskandari also showed that an interphase with higher elastic modulus and yield strength could promote debonding at the fiber–matrix interface leading to degraded composite properties. Related to this, Cheeseman and Santare had shown that the interphase stiffness can either promote or suppress cracking at the fiber–matrix interface depending on the type of fracture [59].

In contrast to significant evidence that a stiffer interphase region promotes overall composite stiffness, there is experimental data that supports the use of a compliant interphase to promote composite toughness through introducing energy dissipation mechanism. Ranade *et al.* showed that an ultra-high molecular weight polyethylene (UHMWPE) coating enhanced the fracture toughness of glass particle filled epoxy composites. The

UHMWPE coating had a lower yield strength than the polymer matrix and led to extrinsic toughening mechanisms by interphasial yielding. However, the introduction on a softer interphase caused a decrease in overall flexural modulus [19]. An alternative approach for simultaneously improving the strength and toughness of composites is by grafting hyper-branched or hierarchical polymer chains on to the fibers, as reviewed by Karger-Kocsis *et al.* [60]. For example, Deng *et al.* grafted diblock copolymers on carbon fibers to simultaneously enhance toughness and strength in carbon-fiber reinforced epoxy composites [18].

Our current study has demonstrated the use of POSS as a carbon fiber surface treatment to greatly enhance the interfacial properties. This effect is greatly affected by the POSS density and bonding between the fiber surface as we have demonstrated previously. The use of a multilayer POSS coating could be used to enhance the properties of the composite even further [12]. Ma and co-workers performed such a study on the effects of multiple layers of POSS on the surface of carbon fibers. The results of this study showed that increasing the number of layers of POSS led to an increase in the interfacial properties. The treatments saw an initial increase of 46% compared to the as-received but by the third POSS layer, the interfacial shear strength had increased to 75% compared to the as-received fibers. Ma and co-workers attributed the increased to the chemical interactions, mechanical interlocking and resin wettability, similar to other research on grafting polymers on reinforcement fibers [18, 48].

The interfacial shear strength appears to increase from each additional layer of POSS. However, Mishra *et al.* in 2017 reported the formation of POSS–POSS agglomerates [37]. These agglomerates would form compliant domains along the fiber surface and result in nonuniform properties at the interface. Therefore, if multiple layers of POSS are to be used, it becomes necessary to limit these agglomerates formation and promote a uniform multilayer coating. This could result in greater increase in interfacial properties than what was seen from Ma and co-workers.

To date there has not been an attempt to control the POSS–POSS networks to ensure

uniform properties across the fiber surface but also control the compliance to tailor the properties of the interface. To this end, this study focuses on generating 3D hierarchical POSS–POSS networks and determine their properties as a function of structure. In the future these POSS–POSS networks would be used as treatments on carbon fibers in composites.

3.2 Materials and methodology

Octavinyl-POSS was purchased from Hybrid Plastics (Hybrid Plastics, Hattiesburg, Mississippi). hexane-1,6-dithiol, 2,2-Dimethoxy-2-phenylacetophenone were supplied by Fisher Chemicals (Fisher Scientific, Pittsburgh, Pennsylvania). Tetrahydrofuran (THF) was supplied by EMD Chemicals (EMD Chemicals, Burlington, Massachusetts) and the UV hand Lamp was purchased through VWR (VWR, Radnor, Pennsylvania). EPOFIX resin and EPOXFIX hardener were purchased from Struers (Struers, Copenhagen, Denmark).

3.2.1 Synthesis of POSS–POSS network

The control of the compliance of these POSS–POSS networks is explored by generating networks of POSS with different cross-linking densities. This will allow us to predict the expected compliance based on the number of POSS–POSS bonds. The steric hindrance will play a role in the number of POSS–POSS connections that are possible as the number of POSS layers are increased. The 3D model of POSS is shown in Figure 3.1. Due to this, when POSS is bound to the surface of the carbon fiber, it would not be possible for all of the eight functional groups to participate in the reaction that will make up the second layer. Based on Figure 3.2 it can be hypothesized that at a maximum, only four of the possible seven free reaction sites will react with the next layer of POSS.

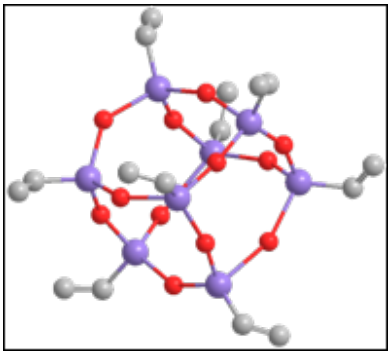

Figure 3.1: 3D model of POSS.

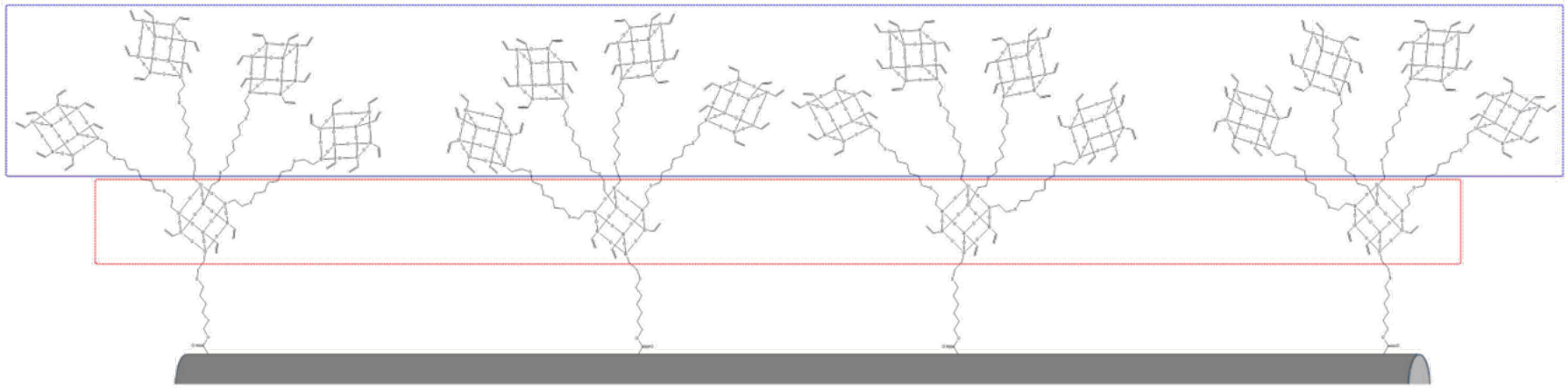

Figure 3.2: Model of a second layer of POSS, bound to the surface of a carbon fiber with an inset of a 3D model of POSS. The initial layer is highlighted by a red square and the second layer is highlighted by a blue square.

The addition of a third layer, it can be expected that the number of POSS would decrease further due to the entanglement from other POSS molecules. The second layer of POSS will likely react with at most two other POSS but some may not contribute at all to building the third layer. This is shown in Figure 3.3 where you can see in the third layer, highlighted by a green box, there are multiple POSS in the second layer that have no POSS reacted with it to make up the third layer. Instead we see that the POSS furthest from the initial layer are able to react with only a few other POSS.

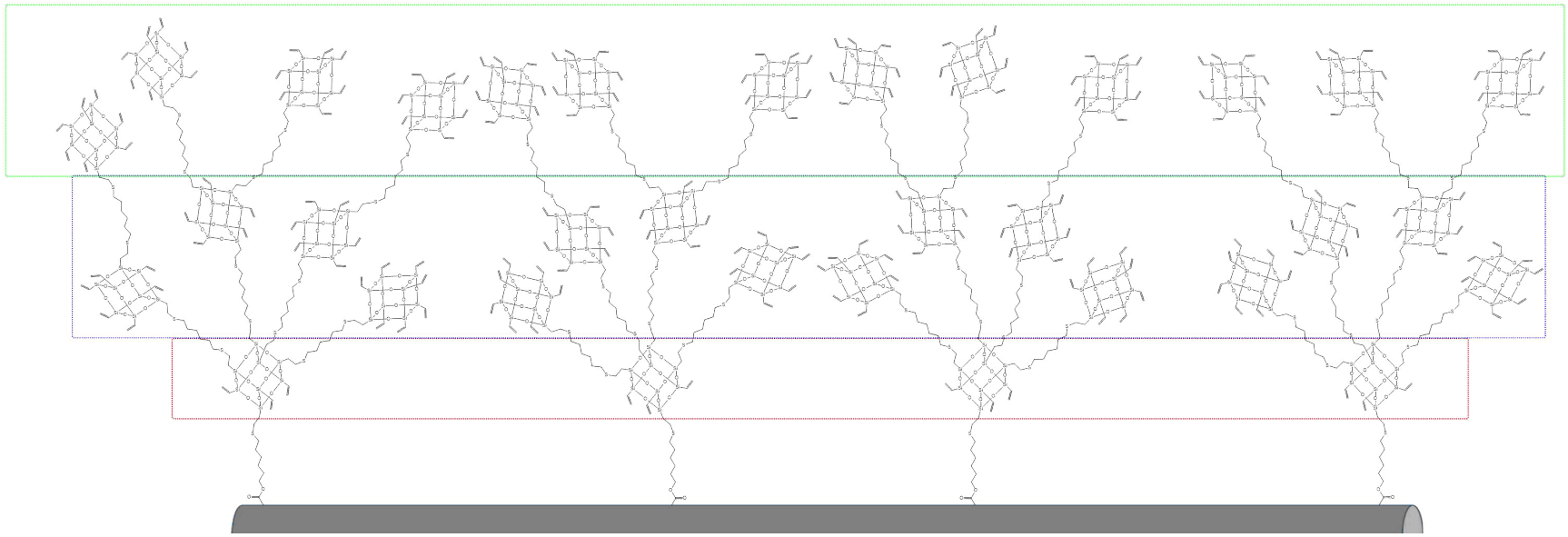

Figure 3.3: Model of a third layer of POSS, bound to the surface of a carbon fiber with an inset of a 3D model of POSS.

To examine the effect of these different POSS densities, four POSS network densities will be synthesized using the following ratios of POSS to the dithiol linker, hexane-1,6-dithiol, 1:0.5, 1:1, 1:2.5 and 1:5. The generic reaction scheme is shown below in Figure 3.4, and the concentration of dithiol will be altered to represent different POSS densities.

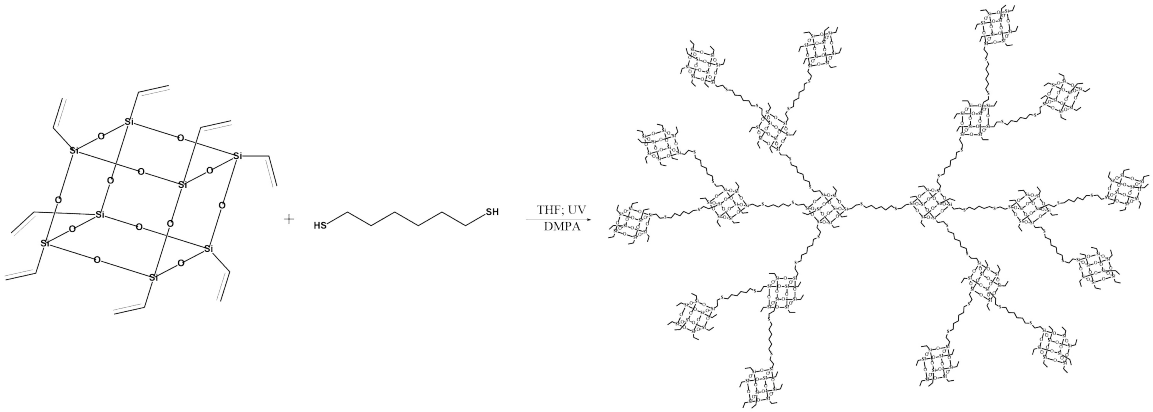

Figure 3.4: Synthesis of POSS–POSS network.

3.2.2 Characterization techniques

Determining the steric hindrance effect caused from the bulky nature of POSS was done using x-ray fluorescence spectroscopy (XRF). XRF is used for the elemental analysis of the POSS–POSS networks. The known structure of the two reactant materials allow us to determine the number of POSS that have reacted. This is done by determining the ratio of silicon to sulfur atoms in the material. The octavinyl-POSS contains eight silicon atoms and the hexane-1,6-dithiol has two sulfur atoms, therefore, by using the XRF to determine the ratios of silicon to sulfur we can estimate the number of POSS–POSS connections. Using this and our known starting ratios used to synthesize each network, we can determine the effect of steric hindrance. Sample requirements for XRF mean that the POSS–POSS networks had to be ground into a fine powder. Unfortunately the 1:5 ratio network, which was the most compliant, was unable to be ground into a powder. The other three samples were ground into a fine powder and placed into a specimen holder ready for XRF.

The determination of the elastic modulus of our synthesized POSS–POSS network will

be done using atomic force microscopy (AFM). AFM can determine the elastic modulus directly once calibrated using a known material typically an epoxy-based material. The epoxy-based material selected is known as EPOFIX, will be used to hold our POSS–POSS material and serve as the calibration material. This requires that the elastic modulus of the EPOFIX material be determined accurately. Samples of EPOFIX epoxy were made by mixing EPOFIX resin and EPOFIX hardener, and poured into molds to make cylindrical samples whose dimensions follow ASTM D695 in order to determine the compressive stress of the material. Prior to testing, samples were speckled for analysis by Digital imagine Correlation (DIC), DIC was used in to determine the full-field strain values of the EPOFIX material, the results of the compressive and DIC tests are shown below in Figure 3.5. This provided the most accurate information to calibrate the AFM and thus provided the most accurate elastic modulus of our POSS–POSS material. The elastic modulus of the EPOFIX was determined to be 2.28 GPa, after an average of three samples were tested. This allowed us to prepare the samples by embedding them into the EPOFIX, and calibrating the AFM to analyze the elastic modulus of the POSS–POSS networks accurately.

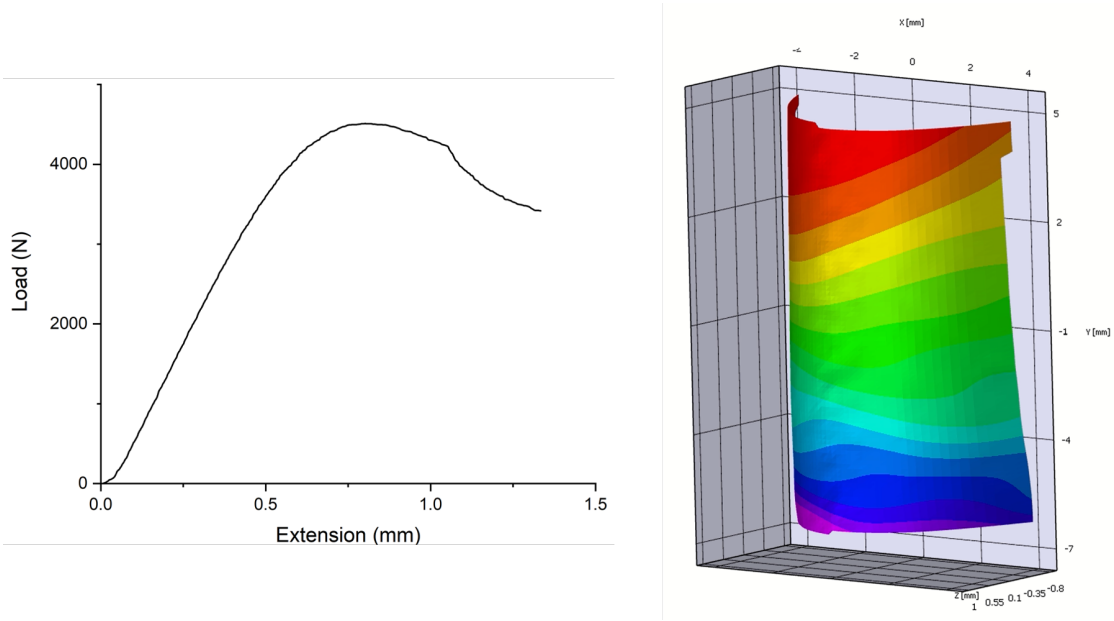

Figure 3.5: On the left is the graph of the compression test used to determine the stress on the sample, on the right is the DIC image, DIC was used to determine the strain on the sample.

3.3 Results and discussion

3.3.1 Determination of the number of POSS–POSS connections within the networks

The results of the XRF for the POSS to dithiol ratios, 1:0.5, 1:1, and 1:2.5m, help determine at what point we see saturation of the POSS–POSS connections, which can be affected by the steric hindrance. The octavinyl-POSS contains eight silicon atoms and the dithiol linking molecule contains two sulfur atoms, therefore for each increase in the ratio we expect to see a proportional decrease in the silicon to sulfur content. The results of the three POSS–POSS networks are shown in Table 3.1. In the first network (1:0.5) it is expected that not all of the POSS molecule will react with another POSS due to the lack of dithiol linker. It is seen that the ratio of silicon to sulfur is 4.0, which is lower than the expected eight silicon to one sulfur (two sulfur multiplied by the 0.5 ratio). However, as we double the ratio from 0.5 to 1 POSS to dithiol, the ratio of silicon to sulfur decreases by half as expected. Lastly, when the POSS to dithiol was increased further to 2.5, the ratio only

decreased by half and signified the steric hindrance effect. This suggests that although there is eight possible functional groups on POSS for connections to form, the bulky nature of POSS is already limiting these connections at a ratio of only 1:2.5 (POSS to dithiol) suggesting this effect will play a large role in formation of additional layers of POSS on the surface of the carbon fiber.

Table 3.1: Results of XRF used to determine the number of POSS–POSS connections.

POSS to Dithiol Ratio	[Si]	[S]	[Si]/[S]
1:0.5	80	20	4.0
1:1	67	33	2.0
1:2.5	49	51	0.96

3.3.2 Determination of elastic modulus of POSS–POSS networks

The different POSS–POSS materials were embedded into the EPOFIX and cured over night. These specimens were sectioned off and polished starting at 400 grit up to 1200 grit to ensure a smooth surface for AFM. The samples were placed in the AFM unit and the tip was placed far from the POSS sample and calibrated using the EPOFIX until a consistent modulus of roughly 2.28 GPa was found at several areas across the sample. Once the calibration was complete, the AFM tip was placed onto the POSS–POSS material and scanned in several areas using the earlier calibration parameters. The Average force data from each force map are shown in Table 3.2. These results show how increasing in ratio of dithiol linker, and as a result the number of POSS–POSS links within the network, impacts the elastic modulus of the material. This demonstrates that by controlling the degree of POSS–POSS connections it is possible to control the stiffness of the interface.

Table 3.2: Results of atomic force microscopy to determine the elastic modulus of different cross-link densities of POSS–POSS networks.

POSS to Dithiol Ratio	Elastic Modulus (GPa)
1:0.5	2.06 ± 3.8
1:1	1.65 ± 0.6
1:2.5	0.95 ± 0.3
1:5	0.42 ± 1.3

The AFM data shows how these POSS–POSS networks can be tuned to achieve a certain compliancy in the interphase. Next, it is necessary to determine what level of compliancy is optimal for the epoxy matrix and IM-7 carbon fibers. Several researchers have attempted to model the properties of composites, including the interphase properties. These are typically done through molecular dynamic (MD) simulations to predict the interaction between the polymer matrix and carbon fiber surface or simply focus on characterizing a particular interphase rather than attempting to determine what is optimal based on a particular fiber and matrix material [61–63]. Eskandari *et al.*, however, developed equation 10 for predicting the optimal shear modulus of the interphase region,(C^i), based on the properties of a selected fiber and matrix material [16]. This will allow us to determine the optimal shear modulus for our select epoxy and carbon fiber system, then compare to our experimental data.

$$(C^i)^2 + \frac{(-C^m + C^f)\left(1 + \frac{r_i^2}{r_f^2}\right)}{\frac{r_i^2}{r_f^2} - 1} C^i - C^f C^m = 0 \tag{10}$$

Where C^m and C^f are the shear modulus of the matrix and the fiber, respectively. r_i and r_f and the radius of the interphase and the fiber, respectively. SEM was used earlier to determine the diameter of the fibers, 5.25μm, and gives a r_f of 2.6μm. Babu *et al.*

determined that the width of interphase in carbon fiber reinforced epoxy is approximately 250 nm thick, we can add that to the fiber radius to get a r_i of 2.85μm [64]. To determine the shear modulus of the fiber and matrix, assuming isotropic behavior, equation 11 can be used.

$$C = \frac{E}{2(1+\nu)} \tag{11}$$

Where C is the shear modulus, E is the elastic modulus and ν is the Poisson's ratio. Kallivokas *et al.* examined the EPON-862 resin system that was used in this work and found it has a elastic modulus of 2.56 GPa and a Poisson's ratio of 0.35, resulting in a C^m value of 0.95 GPa [61]. Lastly, a data sheet from Hexcel on the IM-7 carbon fibers show an elastmic modulus of 276 GPa and a Poisson's ratio of 0.34, these numbers were confirmed by Melo *et al.* [65, 66]. This results in a C^f value of 103 GPa.

These values can be plugged into the above equation from Eskandari *et al.* resulting in the quadratic equation 12. Solving for C^i gives us the optimal interphase shear modulus of 0.09 GPa.

$$(C^i)^2 + 1112.5C^i - 97.9 = 0 \tag{12}$$

To determine the shear modulus of our POSS–POSS networks, denoted C^p, a Poisson's ratio of 0.5 is assumed and the elastic modulus E was determined prior using AFM. The shear modulus of the POSS networks were determined using equation 11 and the results for each ratio of POSS to dithiol are shown below in Table 3.3. The results show a continued drop in Poisson's ratio as we increase the number of POSS–POSS connections.

Table 3.3: Shear modulus of the different POSS–POSS networks.

POSS to Dithiol Ratio	Elastic Modulus (GPa)	Shear Modulus (GPa)
1:0.5	2.06 ± 3.8	0.69
1:1	1.65 ± 0.6	0.55
1:2.5	0.95 ± 0.3	0.32
1:5	0.42 ± 1.3	0.14

3.4 Conclusion and future work

This work demonstrates the ability to control stiffness of the interface by varying the ratio of POSS to dithiol linker. The ability to control the stiffness of the interface can result in overall changes to the properties of a composite. The data shows that the as we increase the ratio of dithiol, subsequently increasing the number of POSS–POSS connections, the material becomes more compliant. However, steric hindrance as a result of the bulky structure of POSS will limit the number of POSS–POSS connections that can be made. This steric hindrance may also lead to unreacted dithiol molecules present in the layers of POSS. These freely moving carbon chains can increase the compliance of the interfacial area. Therefore to limit this, it was important to determine at what point we could expect to see the effects of steric hindrance. Our results show that already at a ratio of POSS to dithiol of 1:2.5, we see some effect of the steric hindrance. This can be used as a way to further increase compliance or used to more accurately synthesize these POSS layers on the surface of the carbon fiber. A optimal shear modulus was determined for the interphase layer and although low at 0.09 GPa, it gives some idea to the number of POSS layers that will be required based on our POSS–POSS experimental data.

In a follow–up study, there are some limitations in the study that should be addressed. These limitations start with the number of tensile tests used in the determination of the Weibull modulus. The Weibull modulus plays a role in the interfacial shear strength calcu-

lation, therefore a more accurate Weibull modulus would result in more confidence in the interfacial shear strength calculation. The same can be said of the number of single–fiber fragmentation tests that were performed. Sample preparation for these single–fiber fragmentation tests is extremely difficult, making large data sets difficult to obtain. There is also a high number of samples that are unusable due to fiber movement during the curing process. Several dozen of each fiber condition were made, however, there were only five test specimens that were analyzed using our testing setup. While towards the end of this study, I had fine tuned the microscope and sample preparation process, this experiment is still extremely tedious. In a future study it would be beneficial to analyze a large batch of samples for each fiber condition, this should be easier with the setup and procedure already in place. Another area that could be addressed in this study are the SEM images, the contour of the fiber make surface analysis through SEM difficult. A more experienced individual may be able to improve the quality of these images with enough time or possibly coating the fiber with a conductive material. The next study should focus on extending the analysis of the multilayer POSS experiments in the AFM and XRD. The data gathered helps show how POSS density impacts the compliance of the material, however, more analysis is needed to understand the mechanics behind this should be explored. Finally, a multilayer POSS–coating of the carbon fibers should then occur and analysis of the mechanical and chemical properties should be repeated and compared to this study of a single layer treatment. The optimal shear modulus determined in this study is quite low. The optimal shear modulus determined in this study used number from literature, it would be more accurate to determine the needed data directly from the carbon fiber and epoxy used in our study. This may result in more accurate determination of an "optimal" interphase region. The changes in compliance in this study were based on POSS density within a network, as opposed to layered on the surface of a carbon fiber. When POSS is layered on the surface of the fiber, the elastic modulus may vary from the experimental data of these networks. It will be important to repeat these studies on fibers coated with multiple layers of POSS.

BIBLIOGRAPHY

[1] Z. Dai, F. Shi, M. Li, and Z. Zhang. Effect of sizing on carbon fiber surface properties and fibers/epoxy interfacial adhesion. *Applied Surface Science*, 257:6980–6985, 2011.

[2] M. Li, H. Liu, Y. Gu, Y. Li, and Z. Zhang. Effects of carbon fiber surface characteristics on interfacial bonding of epoxy resin composite subjected to hygrothermal treatments. *Applied Surface Science*, 288:666–672, 2014.

[3] T. Brocks, M. O. H. Cioffi, and H. J. C. Voorwald. Effect of fiber surface on flexural strength in carbon fabric reinforced epoxy composites. *Applied Surface Science*, 274:210–216, 2013.

[4] B. E.B. Uribe, E. M.S. Chiromito, A. J.F. Carvalho, R. Arenal, and J. R. Tarpani. TEMPO-oxidized cellulose nanofibers as interfacial strengthener in continuous-fiber reinforced polymer composites. *Materials and Design*, 133:340–348, 2017.

[5] H. K. Shin, M. Park, H. Kim, and S. Park. An overview of new oxidation methods for polyacrylonitrile-based carbon fibers. *Carbon letters*, 16(1):11–18, 2015.

[6] M. Sharma, S. Gao, E. Mäder, H. Sharma, L. Y. Wei, and J. Bijwe. Carbon fiber surfaces and composite interphases. *Composites Science and Technology*, 102:35–50, 2014.

[7] G. Wu, L. Ma, Y. Wang, L. Liu, and Y. Huang. Interfacial properties and impact toughness of methylphenylsilicone resin composites by chemically grafting POSS and tetraethylenepentamine onto carbon fibers. *Composites Part A: Applied Science and Manufacturing*, 84:1–8, 2016.

[8] S. Tiwari and J. Bijwe. Surface Treatment of Carbon Fibers - A Review. *Procedia Technology*, 14:505–512, 2014.

[9] X. Z. Zhang, Y. J. Song, and Y. D. Huang. Properties of silsesquioxane coating modified carbon fibre/polyarylacetylene composites. *Composites Science and Technology*, 67(14):3014–3022, 2007.

[10] J. Moosburger-Will, M. Bauer, E. Laukmanis, R. Horny, D. Wetjen, T. Manske, F. Schmidt-Stein, J. Töpker, and S. Horn. Interaction between carbon fibers and polymer sizing: Influence of fiber surface chemistry and sizing reactivity. *Applied Surface Science*, 439:305–312, 2018.

[11] R. L. Zhang, J. S. Zhang, L. H. Zhao, and Y. L. Sun. Sizing agent on the carbon fibers surface and interface properties of its composites. *Fibers and Polymers*, 16(3):657–663, 2015.

[12] L. Ma, Y. Zhu, M. Wang, X. Yang, G. Song, and Y. Huang. Enhancing interfacial strength of epoxy resin composites via evolving hyperbranched amino-terminated POSS on carbon fiber surface. *Composites Science and Technology*, 170:148–156, 2019.

[13] M. Yourdkhani, W. Liu, S. Baril-gosselin, F. Robitaille, and P. Hubert. Carbon nanotube-reinforced carbon fibre-epoxy composites manufactured by resin film infusion. *Composite Science and Technology*, 166:169–175, 2018.

[14] P. Y. Hung, K. T. Lau, B. Fox, N. Hameed, J. H. Lee, and D. Hui. Surface modification of carbon fibre using graphene–related materials for multifunctional composites. *Composites Part B: Engineering*, 133:240–257, 2018.

[15] K. S. Khare, F. Khabaz, and R. Khare. Effect of carbon nanotube functionalization on mechanical and thermal properties of cross-linked epoxy-carbon nanotube nanocom-

posites: Role of strengthening the interfacial interactions. *ACS Applied Materials and Interfaces*, 6(9):6098–6110, 2014.

[16] S. Eskandari, G. Carman, and S. Case. Evaluating the Influence of Fiber Coatings on the Compression Strength of a Unidirectional Polymer Composite. *Journal of Composite Materials*, 30(18):1958–1976, 1996.

[17] A. Needleman, T. L. Borders, L. C. Brinson, V. M. Flores, and L. S. Schadler. Effect of an interphase region on debonding of a CNT reinforced polymer composite. *Composites Science and Technology*, 70(15):2207–2215, 2010.

[18] S. H. Deng, X. D. Zhou, M. Q. Zhu, C. J. Fan, and Q. F. Lin. Interfacial toughening and consequent improvement in fracture toughness of carbon fiber reinforced epoxy resin composites: Induced by diblock copolymers. *Express Polymer Letters*, 7(11):925–935, 2013.

[19] R. A. Ranade, J. Ding, S. L. Wunder, and G. R. Baran. UHMWPE as interface toughening agent in glass particle filled composites. *Composites Part A: Applied Science and Manufacturing*, 37(11):2017–2028, 2006.

[20] S. Tiwari, J. Bijwe, and S. Panier. Tribological studies on polyetherimide composites based on carbon fabric with optimized oxidation treatment. *Wear*, 271(9-10):2252–2260, 2011.

[21] C. Pramanik, D. Nepal, M. Nathanson, J. R. Gissinger, A. Garley, R. J. Berry, A. Davijani, S. Kumar, and H. Heinz. Molecular engineering of interphases in polymer/carbon nanotube composites to reach the limits of mechanical performance. *Composites Science and Technology*, 166:86–94, 2018.

[22] X. Yao, X. Gao, J. Jiang, C. Xu, C. Deng, and J. Wang. Comparison of carbon nanotubes and graphene oxide coated carbon fiber for improving the interfacial properties

of carbon fiber/epoxy composites. *Composites Part B: Engineering*, 132:170–177, 2018.

[23] J. Zhu, A. Imam, R. Crane, K. Lozano, V. N. Khabashesku, and E. V. Barrera. Processing a glass fiber reinforced vinyl ester composite with nanotube enhancement of interlaminar shear strength. *Composites Science and Technology*, 67(7-8):1509–1517, 2007.

[24] M. Zhao, L. Meng, L. Ma, L. Ma, X. Yang, Y. Huang, J. Ryu, A. Shankar, T. Li, C. Yan, and Z. Guo. Layer-by-layer grafting CNTs onto carbon fibers surface for enhancing the interfacial properties of epoxy resin composites. *Composites Science and Technology*, 154:28–36, 2018.

[25] B. Gao, R. Zhang, M. He, L. Sun, C. Wang, L. Liu, L. Zhao, H. Cui, and A. Cao. Effect of a multiscale reinforcement by carbon fiber surface treatment with graphene oxide/carbon nanotubes on the mechanical properties of reinforced carbon/carbon composites. *Composites Part A: Applied Science and Manufacturing*, 90:433–440, 2016.

[26] E. Bekyarova, E. Thostenson, A. Yu, M. Itkis, D. Fakhrutdinov, T. Chou, and R. Haddon. Functionalized Single-Walled Carbon Nanotubes for Carbon Fiber-Epoxy Composites. *J. Phys. Chem.*, 111:17865–17871, 2007.

[27] K. Lau, M. Lu, and K. Liao. Improved mechanical properties of coiled carbon nanotubes reinforced epoxy nanocomposites. *Composites Part A: Applied Science and Manufacturing*, 37(10):1837–1840, 2006.

[28] T. Kamae and L. T. Drzal. Carbon fiber/epoxy composite property enhancement through incorporation of carbon nanotubes at the fiber-matrix interphase - Part I: The development of carbon nanotube coated carbon fibers and the evaluation of their ad-

hesion. *Composites Part A: Applied Science and Manufacturing*, 43(9):1569–1577, 2012.

[29] M. Li, Y. Gu, Y. Liu, Y. Li, and Z. Zhang. Interfacial improvement of carbon fiber/epoxy composites using a simple process for depositing commercially functionalized carbon nanotubes on the fibers. *Carbon*, 52:109–121, 2013.

[30] A. A. Shvedova, E. R. Kisin, R. Mercer, A. R. Murray, V. J. Johnson, A. I. Potapovich, Y. Y. Tyurina, O. Gorelik, S. Arepalli, D. Schwegler-Berry, A. F. Hubbs, J. Antonini, D. E. Evans, B. K. Ku, D. Ramsey, A. Maynard, V. E. Kagan, V. Castranova, and P. Baron. Unusual inflammatory and fibrogenic pulmonary responses to single-walled carbon nanotubes in mice. *American Journal of Physiology - Lung Cellular and Molecular Physiology*, 289(5):698–708, 2005.

[31] R. R. Mercer, A. F. Hubbs, J. F. Scabilloni, L. Wang, L. A. Battelli, S. Friend, V. Castranova, and D. W. Porter. Pulmonary fibrotic response to aspiration of multi-walled carbon nanotubes. *Particle and Fibre Toxicology*, 8:21, 2011.

[32] CDC Department of Health and human servies. Occupational exposure to carbon nanotubes and nanofibers. Technical report, 2014.

[33] E. Ayandele, B. Sarkar, and P. Alexandridis. Polyhedral Oligomeric Silsesquioxane (POSS)-Containing Polymer Nanocomposites. *Nanomaterials*, 2(4):445–475, 2012.

[34] S. W. Kuo and F. C. Chang. POSS related polymer nanocomposites. *Progress in Polymer Science (Oxford)*, 36(12):1649–1696, 2011.

[35] J. J. Schwab and J. D. Lichtenhan. Polyhedral Oligomeric Silsesquioxane (POSS)-Based Polymers. *Applied Organometallic Chemistry*, 12(10-11):707–713, 1998.

[36] M. Sánchez-Soto, D. A. Schiraldi, and S. Illescas. Study of the morphology and properties of melt-mixed polycarbonate-POSS nanocomposites. *European Polymer Journal*, 45(2):341–352, 2009.

[37] K. Mishra, G. Pandey, and R. P. Singh. Enhancing the mechanical properties of an epoxy resin using polyhedral oligomeric silsesquioxane (POSS) as nano-reinforcement. *Polymer Testing*, 62:210–218, 2017.

[38] K. Mishra, L. K. Babu, and R. Vaidyanathan. Improvement of fracture toughness and thermo-mechanical properties of carbon fiber/epoxy composites using polyhedral oligomeric silsesquioxane. *Journal of Composite Materials*, 54(10):1273–1280, 2020.

[39] R. L. Zhang, C. G. Wang, L. Liu, H. Z. Cui, and B. Gao. Polyhedral oligomeric silsesquioxanes/carbon nanotube/carbon fiber multiscale composite: Influence of a novel hierarchical reinforcement on the interfacial properties. *Applied Surface Science*, 353:224–231, 2015.

[40] D. Jiang, L. Xing, L. Liu, X. Yan, J. Guo, X. Zhang, Q. Zhang, Z. Wu, F. Zhao, Y. Huang, S. Wei, and Z. Guo. Interfacially reinforced unsaturated polyester composites by chemically grafting different functional POSS onto carbon fibers. *Journal of Materials Chemistry A*, 2(43):18293–18303, 2014.

[41] G. Wu, L. Ma, H. Jiang, and L. Liu. Directly grafting octa (aminophenyl) polyhedral oligomeric silsesquioxane onto carbon fibers for superior interfacial strength and hydrothermal aging resistance of silicone resin composites. *Construction and Building Materials*, 157:1040–1046, 2017.

[42] E. Werner. The preparation of ethylamine and of diethylamine. *J. Chem. Soc.*, (113):899–902, 1918.

[43] H. C. Kolb, M. G. Finn, and K. B. Sharpless. Click Chemistry: Diverse Chemical Function from a Few Good Reactions. *Angewandte Chemie - International Edition*, 40(11):2004–2021, 2001.

[44] P. Lundberg, C. J. Hawker, A. Hult, and M. Malkoch. Click assisted one-pot multi-step reactions in polymer science: Accelerated synthetic protocols. *Macromolecular Rapid Communications*, 29(12-13):998–1015, 2008.

[45] W. Binder and C. Kluger. Azide/Alkyne-"Click" Reactions: Applications in Material Science and Organic Synthesis. *Current Organic Chemistry*, 10(14):1791–1815, 2006.

[46] C. E. Hoyle and C. N. Bowman. Thiol-ene click chemistry. *Angewandte Chemie - International Edition*, 49(9):1540–1573, 2010.

[47] C. Kuttner, M. Tebbe, H. Schlaad, I. Burgert, and A. Fery. Photochemical synthesis of polymeric fiber coatings and their embedding in matrix material: Morphology and nanomechanical properties at the fiber-matrix interface. *ACS Applied Materials and Interfaces*, 4(7):3484–3492, 2012.

[48] C. Kuttner, A. Hanisch, H. Schmalz, M. Eder, H. Schlaad, I. Burgert, and A. Fery. Influence of the polymeric interphase design on the interfacial properties of (fiber-reinforced) composites. *ACS Applied Materials and Interfaces*, 5(7):2469–2478, 2013.

[49] I. Ibrahim, S. Sarip, N. A. Bani, M. H. Ibrahim, and M. Z. Hassan. The Weibull probabilities analysis on the single kenaf fiber. *AIP Conference Proceedings*, 1958, 2018.

[50] S. Feih, K. Wonsyld, D. Minzari, P. Westermann, and H. Lilholt. *Testing procedure for the single fiber fragmentation test*, volume 1483. 2004.

[51] Y. Yilmaz. Analyzing Single Fiber Fragmentation. *Journal of Composite Materials*, 36(5):537–551, 2002.

[52] Y. Swolfs, I. Verpoest, and L. Gorbatikh. Issues in strength models for unidirectional fibre-reinforced composites related to Weibull distributions, fibre packings and boundary effects. *Composites Science and Technology*, 114:42–49, 2015.

[53] F. Mesquita, Y. Swolfs, S. Bucknell, Y. Leray, S. V. Lomov, and L. Gorbatikh. Tensile Properties of Single Carbon Fibres Tested With Automated Equipment. *Iccm22*, 2019.

[54] Y. Yang, W. Li, W. Tang, B. Li, and D. Zhang. Sample sizes based on weibull distribution and normal distribution for FRP tensile coupon test. *Materials*, 12(1):1–10, 2019.

[55] F. Wang and J. Shao. Modified Weibull distribution for analyzing the tensile strength of bamboo fibers. *Polymers*, 6(12):3005–3018, 2014.

[56] C. T. Rueden, J. Schindelin, and M. C. Hiner. ImageJ, 2017.

[57] J. D. Achenbach and H. Zhu. Effect of interfacial zone on mechanical behavior and failure of fiber-reinforced composites. *Journal of the Mechanics and Physics of Solids*, 37(3):381–393, 1989.

[58] L. T. Drzal. The role of the fiber-matrix interphase on composite properties. *Vacuum*, 41(7-9):1615–1618, 1990.

[59] B. A. Cheeseman and M. H. Santare. The effect of the interphase on crack-inclusion interactions. *International Journal of Fracture*, 109(3):303–323, 2001.

[60] J. Karger-Kocsis, H. Mahmood, and A. Pegoretti. Recent advances in fiber/matrix interphase engineering for polymer composites. *Progress in Materials Science*, 73:1–43, 2015.

[61] S. V. Kallivokas, A. P. Sgouros, and D. N Theodorou. Molecular dynamics simulations of EPON-862/DETDA epoxy newtorks: structure, topology, elastic constrants, and local dynamics. *Soft Matter*, 15:721–733, 2019.

[62] O. K. Buryan and V. U. Novikov. Modeling of the Interphase of Polymer-Matrix Composites: Determination of Its Structure and Mechanical Properties. *Mechanics of Composite Materials*, 38(3):187–198, 2002.

[63] K. Antin, A. Laukkanen, T. Andersson, D. Smyl, and P. Vilaca. A Multiscale Modelling Approach for Estimating the Effect of Defects in Unidirectional Carbon Fiber Reinforced Polymer Composites. *Materials*, 12:1885, 2019.

[64] L. K. Babu, K. Mishra, and R. P. Singh. Near–fiber effects of UV irradiation on the fiber–matrix interphase: A combined experimental and numerical investigation. *Materials and Design*, 157:294–302, 2018.

[65] K. Marlett. Hexcel 8552 IM7 Unidirectional Prepreg 190 gsm & 35%RC Qualification Material Property Data Report. Technical report, National Institute for Aviation Research, 2011.

[66] J. D. Melo and D. W. Radford. Elastic characterization of PEEK / IM7 using coefficients of thermal expansion. *Composites Part A: Applied Science and Manufacturing*, 33:1505–1510, 2002.

VITA

Blaze Allan Heckert

Candidate for the Degree of

Doctor of Philosophy

Dissertation: POSS-BASED CARBON FIBER TREATMENT FOR ENHANCED STRENGTH AND TOUGHNESS OF COMPOSITES

Major Field: Materials Science and Engineering

Biographical:

Education:

Completed the requirements for the Doctor of Philosophy in Materials Science and Engineering at Oklahoma State University, Stillwater, Oklahoma in July, 2020.

Completed the requirements for the Master of Science in Polymer Chemistry at Pittsburg State University, Pittsburg, Kansas in May, 2016.

Completed the requirements for the Bachelor of Science in Biology at Pittsburg State University, Pittsburg, Kansas in May, 2015.

Experience: Worked as a Graduate Research Assistant at the Mechanics of Advanced Materials Laboratory headed by Dr. Raman P. Singh in the area of multifunctional composites.

Worked as a Graduate Research Assistant at thenanotheranostics lab headed by Dr. Santimukul Santra